63-3-2

QUARTERLY PROGRESS REPORT
NUMBER 48 APRIL 15, 1963

(1)

SOLID-STATE AND
MOLECULAR THEORY GROUP

MASSACHUSETTS INSTITUTE
OF TECHNOLOGY
CAMBRIDGE, MASSACHUSETTS

$6.60

SOLID-STATE AND MOLECULAR THEORY GROUP, M.I.T. Q.P.R. No. 48, April 15, 1963

The research reported in this document was made possible through support extended the Massachusetts Institute of Technology, Department of Physics, by the Navy Department (Office of Naval Research), under O.N.R. Contract Nonr-1841(34); by the Army, Navy, and Air Force (Lincoln Laboratory), under Purchase Order P.O. C-00663; by the National Science Foundation, under Grant NSF-G10821; by the Air Force and the Advanced Research Projects Agency (Air Force Cambridge Research Laboratory), under Contract AF 19(628)-356. Reproduction in whole or in part is permitted for any purpose by the United States Government.

QUARTERLY PROGRESS REPORT
NUMBER 48, APRIL 15, 1963

SOLID-STATE AND
MOLECULAR THEORY GROUP

MASSACHUSETTS INSTITUTE
OF TECHNOLOGY

O.N.R. Contract Nonr-1841(34)
Lincoln Laboratory P.O. C-00663
N.S.F. Grant NSF-G24908
~~A.F.C.R.L. Contract AF 19(628)-356~~

Faculty

Professor J. C. Slater, Director
Professor M. P. Barnett
Professor G. F. Koster
Professor J. H. Wood

Staff Members, Research Assistants, Graduate Students

M. J. Bailey
I. G. Csizmedia
J. P. Dahl
P. DeCicco
D. E. Ellis
R. Englman
M. C. Harrison
L. F. Mattheiss
J. Moskowitz
C. Nielson
F. W. Quelle
P. M. Scop
C. M. Sonnenschein
B. T. Sutcliffe
A. C. Switendick
L. Szasz
B. J. Woznick
J. P. Wright

Visiting Fellow

A. J. Freeman*

Secretary

Margaret Viles

*Staff member, National Magnet Laboratory, MIT.

TABLE OF CONTENTS

Quarterly Progress Report No. 48
of
Solid-State and Molecular Theory Group, M.I.T.
including work sponsored by
O.N.R. Contract Nonr-1841(34)
Lincoln Laboratory P.O. C-00663
N.S.F. Grant NSF-G24908
A.F.C.R.L. Contract AF 19(628)-356

SURVEY

At the St. Louis meeting of the American Physical Society, on March 25-28, we are presenting a review of recent work on the energy bands of solids, using the augmented plane wave method. I am giving a half-hour invited paper, followed by contributed papers by Mattheiss, Wood, Switendick, and Pratt, all on topics which have been recently reported in these Quarterly Progress Reports. There are several points which I shall emphasize in my talk, as well as sketching the main ideas of the APW method. One of these points is that the APW method is not tied to the use of a potential which is constant between the atomic spheres, as well as being spherically symmetrical within the spheres. There is no complication involved in having an arbitrary potential in the space between the spheres. All that has to be done is to expand in three-dimensional Fourier series a function equal to the assumed potential between the spheres, and zero within each sphere. The Fourier components of this expansion immediately give contributions to the diagonal and non-diagonal matrix elements of the Hamiltonian between the augmented plane waves, before solving the secular problem, which carries through as usual. This was pointed out in the first paper on the APW method, and has been emphasized particularly in still unpublished work by P. M. Marcus and H. Schlosser (I am indebted to them for pointing this out to me). Though we have not so far used such a Fourier expansion, we are actively exploring its use, and shall expect to use it as soon as we have decided what potential to assume.

A second point which I shall emphasize is that though the energy bands in some metals are rather free-electron like, nevertheless this is not a general situation, and it makes the use of the various pseudo-potential methods which have been proposed very dubious in general. One can approach the problem by considering the logarithmic derivatives of the radial solutions of Schrödinger's equation at the radius of the atomic spheres. If these logarithmic derivatives happened to equal the logarithmic derivatives of the spherical Bessel functions corresponding to free electrons whose energy equalled the actual energy of the

problem, the solution of Schrödinger's equation inside the sphere would join smoothly onto a single plane wave outside the sphere. This would mean that a plane wave solution in the regions between the spheres would not be scattered by the atoms. In such a case one can show that the solution, for this energy, is free-electron like as far as its energy is concerned, as well as having a wave function which is a plane wave except within the spheres. This is the same situation which, in the problem of scattering of a plane wave by an isolated atom, leads to the Ramsauer effect, according to which certain atoms, particularly the inert gas atoms, show practically a zero scattering cross section for slow electrons. The point now is that the logarithmic derivatives for the crystal potentials in such cases as sodium, magnesium, and aluminum have almost exactly this property, leading to the free-electron-like behavior of the energy bands in these cases. In most cases, however, we do not have this situation, and the use of free electron solutions as a starting point is not at all justified. In every case the APW method is applicable, but the only way to test the applicability of pseudo-potential methods is to compare them with more accurate solutions, such as the APW, and if the accurate solution is available, there is no point in using the free-electron approximation.

A further point regarding the APW method is its applicability in many cases where other methods are impossible or difficult. One of these, of course, is the study of the transition series of elements. Another is the study of crystals involving very heavy atoms, in which no particular difficulty arises when using the APW method, as Pratt and his students have shown, but for which the OPW method is rather difficult. For the study of spin-orbit interaction, the APW method is particularly convenient, since the spin-orbit interaction Hamiltonian is zero except where there is an external electric field, which means that if we have the conventional potential used in the APW method, constant between atoms, the Hamiltonian will vanish except within the spheres. Within these spheres, since we have spherical symmetry, we can carry through the ordinary transformation reducing the spin-orbit interaction to an operator involving $\vec{S}\cdot\vec{L}$, the scalar product of spin and orbital angular momentum. Furthermore, the wave function within the spheres is expanded in series of terms each with a fixed angular momentum, so that it is easy to deal with the matrix elements. These advantages have been pointed out in an unpublished memorandum by Larry Johnson, working with Pratt.

I have included this sketch of my remarks at the meeting, since they will not be published elsewhere. As for the new results to be reported, perhaps the most striking are Mattheiss's calculations of energy bands for almost the whole 3d transition series of elements, which he reports in the present Quarterly Progress Report. These are still preliminary results, in that he has so far determined energy bands only in a few directions, but the programs are

working so well that we can now turn out these energy bands very rapidly, and it will not be long before much more complete information is available. It is particularly interesting to check the validity of the rigid band model of the transition elements, to see the gradual narrowing of the 3d bands as we go up in the series, and to see the rapid descent of the 3d bands below the 4s and 4p as we go from copper to zinc and gallium. This is the first time that it has been possible to assemble on a common basis a set of energy band calculations for these elements, including representatives of body- and face-centered cubic and hexagonal structures. Wood's work on gallium fits onto this series, and is entirely consistent with it. The case of gallium, however, is one of the most complicated which we have yet encountered as far as the structure of the Fermi surface is concerned, and it is by now clear that many further points in the Brillouin zone will have to be calculated before the shape of the Fermi surface is entirely clarified. Wood is proceeding with the calculation of these further points.

In the two preceding Quarterly Progress Reports I have presented results on symmetry properties of a number of hexagonal and cubic space groups. I conclude this series with some tetragonal and rhombohedral space groups, in the present Quarterly Progress Report. In the next Quarterly Progress Report, of July 15, 1963, I propose to give some discussion of double space groups, and their relation to spin-orbit interaction.

The work on molecular calculations and molecular integrals has been proceeding rapidly during the preceding quarter, as is shown by no less than seven contributions to this Quarterly Progress Report, by Moskowitz, Sutcliffe, Harrison, Ellis, Wright, Dahl, and Nielson and Woznick. Some of these deal with specific molecules, but most of them are concerned with the calculation of three- and four-center integrals, with mathematical techniques associated with their calculation, and with packages of programs for the calculation of molecular wave functions. Excellent progress is being made with this programming, but there is still quite a way to go before we are ready to make wholesale calculations of polyatomic molecules.

We have one addition to the group since the last Quarterly Progress Report, Dr. J. P. Dahl, from the University of Copenhagen, who will be with the group for approximately a year. Fred Quelle, who has been associated with the group for several years, as a graduate student at Harvard as well as being associated with the Lincoln Laboratory, has now completed his requirements for the doctor's degree at Harvard. He continues to be associated with the Office of Naval Research. Roberts has received his degree since the last Quarterly Progress Report, and has left to take a position at the Bell Telephone Laboratories, Inc.

Professor M. P. Barnett, who has been with us since 1958, has just been appointed to a Readership in Information Processing at the Computer Unit of the University of London, a position in which he will be a senior member in one of the largest computer installations in the world. He will leave in September 1963 to take up his new post. He will leave a serious gap in our group, and arrangements have not yet been made to fill his place, either as Director of the Cooperative Computing Laboratory or as a scientific member of the group. It is our intention, however, to continue the operation of the Cooperative Computing Laboratory along its present lines, which have been so soundly originated by Prof. Barnett, and to continue the work on molecular calculation and molecular integrals. It is our hope that during the remaining months of Prof. Barnett's term here, with the large group now working on the programming problem for the polyatomic molecules, we shall be able to bring this problem to a point where it provides usable methods for the quantitative study of polyatomic molecules.

J. C. Slater

ENERGY BANDS FOR THE IRON TRANSITION SERIES

L. F. Mattheiss

I. Introduction

Energy bands have been calculated for a majority of the elements in the iron transition series using the augmented plane wave (APW) method[1, 2]. While these results are preliminary in nature and not in any sense complete, they may be of some interest to experimentalists and theoreticians who are concerned with the electronic structure of the transition series elements. The present results represent energy bands for three different crystal structures, with a variety of lattice constants. Despite the detailed differences that are imposed by symmetry requirements and variations in lattice constants, the results suggest some interesting and rather clear cut trends in the band structure of these elements as one proceeds through the transition series. These calculations lend some support to the rigid band model for the transition series. They support the hope that systematic studies of the band structure of the transition series elements can provide useful qualitative, and perhaps quantitative, information concerning their electronic structure.

As in all calculations involving d electrons, the results are sensitive to the choice of potentials. The crystal potentials used in these calculations were all constructed in an analogous manner, and were approximated by a superposition of atomic potentials. The method involves the use of Hartree-Fock solutions to the corresponding atomic problem[3] and the free electron exchange approximation[4]. The details of this method for constructing approximate crystal potentials have been described earlier[5], though a brief resume is presented in Section II of this paper, along with other information pertaining to this present series of calculations. The energy bands along a single line of symmetry in the appropriate Brillouin zone are presented in Section III for A, Ti, V, Cr, Fe, Co, Ni, Cu, and Zn, while the last section contains a brief discussion of these results.

II. Description of the Calculations

In these calculations, the crystal potential has been approximated by a superposition of atomic potentials. The coulomb and exchange contributions to the crystal potential are treated separately. An approximate crystal coulomb potential and charge density in a given atomic cell is obtained by expanding the neutral atom coulomb potentials and charge densities of neighboring atoms about the origin, using Löwdin's alpha function expansion[6], keeping only the $\ell = 0$ or spherically symmetric terms in these expansions. Using the free electron exchange approximation, the exchange potential is proportional to the cube root of the superimposed atomic charge densities. It is felt that by using this superimposed charge density, the principal deficiency in the free electron exchange approximation is compensated, namely that it falls off too rapidly at large radii in atomic systems.

The potentials obtained by this method are generally rather flat near the boundaries of the atomic cell, at least in the case of metals, so they are readily approximated by a "muffin-tin" type potential, as required by the APW method. The constant value of the potential outside the APW spheres is taken as the average value of the potential in this region. This usually results in a discontinuity in the potential at the sphere radius amounting to a few hundredths of a Rydberg.

In the construction of approximate crystal potentials for transition series elements, there is frequently some ambiguity in choosing the most reasonable atomic configuration. This sort of difficulty can only be answered satisfactorily by experimental information and/or self consistent energy band calculations. For the present, we have been content to study the effect that changing the atomic configuration has on the band structure. In addition, there are magnetic effects which create additional complications in this series of elements. For simplicity, all magnetic effects have been neglected in these calculations, and the crystals have been assumed to be non-magnetic in character.

The lattice constants which have been used in these calculations have generally been the room temperature values as tabulated in Pearson's book, A Handbook of Lattice Spacings and Structures of Metals and Alloys[7]. The exceptions are those for A and Zn. The lattice constant for A is the low temperature value obtained by Dobbs and Jones[8]. In the case of Zn, Harrison[9] has extrapolated the room temperature lattice constants to low temperatures since the results are expected to be sensitive to the choice of c/a ratio. For purposes of comparison, his values have been used in these calculations. Table 1 contains a summary of the elements considered in these calculations, their structures, the values of the lattice constants, and the assumed atomic configurations.

Table 1

In this table, we list the elements of the iron transition series, their structures, the lattice constants used in this series of calculations (in atomic units), and the assumed atomic configurations.

Element	Structure	a (au)	c (au)	Configuration
A	fcc	10.0346		$(3s)^2(3p)^6$
K				
Ca				
Sc				
Ti	hcp	5.5755	8.8503	$(3d)^3(4s)^1$
V	bcc	5.7225		$(3d)^4(4s)^1$
Cr	bcc	5.4512		$(3d)^5(4s)^1$
Mn				
Fe	bcc	5.4168		$(3d)^7(4s)^1$
Co	fcc	6.6975		$(3d)^8(4s)^1$
Ni	fcc	6.6590		$(3d)^9(4s)^1$
Cu	fcc	6.8309		$(3d)^{10}(4s)^1$
Zn	hcp	5.0120	9.1453	$(3d)^{10}(4s)^2$

III. Results

The principal results of these calculations are presented in Figure 1. These results represent plots of energy as a function of wave vector along lines of symmetry from the center to a boundary of the appropriate Brillouin zones. For the face centered cubic structures (A, Co, Ni, and Cu), the bands are plotted from Γ along the Δ direction to the point X, using the notation of Bouckaert, Smoluchowski, and Wigner[10]. In the body centered cubic structure (V, Cr, and Fe), the bands are plotted from Γ along the Δ direction to the point H. Finally, in the hexagonal close packed structure (Ti and Zn), they start at Γ and proceed along the line T in the $k_z = 0$ plane which terminates at the point K, one of the vertices of the hexagon (in the notation of Herring[11]).

The energy is in Rydbergs and the wave vectors for the different elements are drawn to scale for purposes of comparison. The horizontal dashed lines represent rough estimates of the Fermi energy for each element. For simplicity, some of the more highly excited bands have been omitted in some cases, particularly in the face centered cubic structure, or in other situations, they have been sketched in by dashed lines.

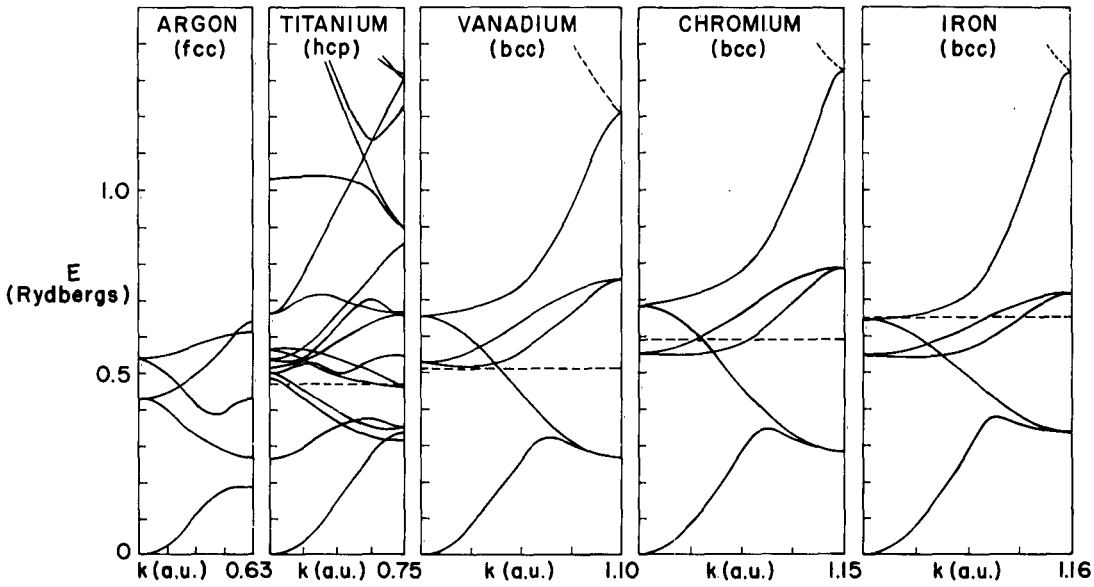

Figure 1

Energy bands for A, Ti, V, Cr, Fe, Co, Ni, Cu, and Zn as a function of wave vector along a line of symmetry in the appropriate Brillouin zones. For the face centered cubic structure, the bands are plotted from Γ along Δ to the point **X**. For the body centered cubic structure, they are plotted

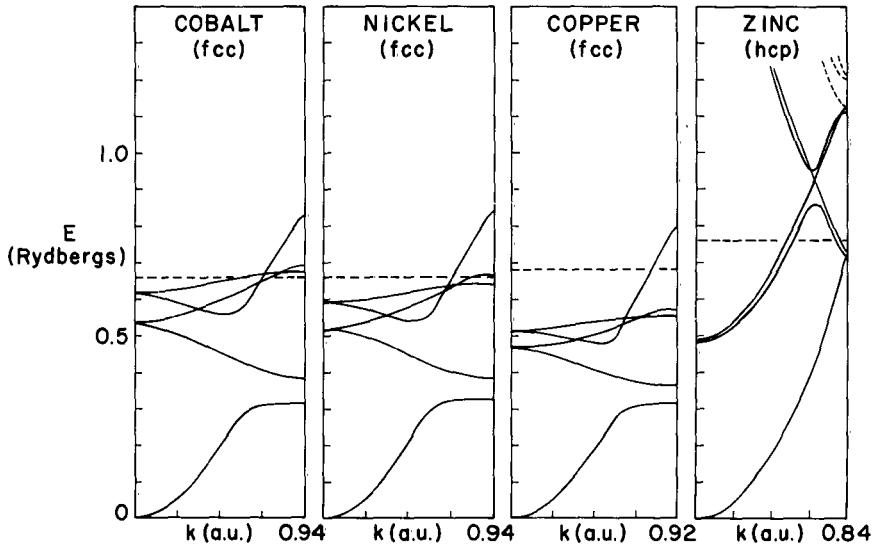

Figure 1 (cont.)

from Γ along Δ to the point H. Finally, for the hexagonal close packed structure, they are plotted from Γ along T to the point K. The energies are in Rydbergs and the wave vectors are in atomic units.

In Figure 2, it is shown what effect varying the atomic configuration has on the band structure of a typical element, namely vanadium. The bands to the right are the ones shown in Figure 1 for vanadium; the ones to the left are those obtained from a potential which results from an atomic configuration containing an additional 4s electron and one less 3d electron. In general, this results in a narrowing of the 3d band and a decrease in the energy separation between the top of the 3d band and the bottom of the 4s-4p bands.

IV. Discussion

In the simplified picture of the energy bands for the iron transition series elements, one finds a narrow 3d band in the midst of a rather broad 4s-4p band. The width of the 3d band and especially its position relative to the bottom of the 4s-4p band depend rather critically on the potential. Nevertheless, the results of Figure 1 exhibit a reasonably smooth variation from element to element, especially for those substances having the same crystal structure. This seems to lend some support to the rigid band model for the transition series elements, an approximation which has been of considerable value in understanding the electronic properties of these elements and their alloys.

There is a gradual narrowing of the 3d band as one progresses through the series. This effect was discussed by Slater in order to explain the occurrence of ferromagnetism in the latter part of the series[12]. In going from Cu to Zn, the 3d band suddenly drops about 0.5 Rydberg below the bottom of the 4s-4p bands, and its width decreases to less than 0.1 Rydberg. As a result, the energy bands for zinc are very free electron-like. For those elements where the 3d band falls in the middle of the 4s-4p bands, the interactions between states having the same symmetry causes considerable modification to the free electron bands, though at points of symmetry, the effect is sometimes small. The bands for Ti and Zn demonstrate this effect nicely.

The results of Figure 2 emphasize the uncertainty which is inherent in any energy band calculation for a transition series element. These uncertainties have been pointed out previously in the literature, particularly by Callaway[13]. These difficulties can only be cleared up satisfactorily with the aid of more detailed experimental information regarding the band structure of these elements in addition to self consistent energy band calculations.

The results presented here are not complete enough to permit detailed comparisons to be made with experiment or a discussion of the resulting Fermi surfaces. However, there are some striking similarities between the energy bands shown in Figure 1 and the results obtained by earlier calculations. In particular, there is good qualitative agreement between the Cu results shown on Figure 1 and the bands calculated by Segall[14] and also by Burdick[15].

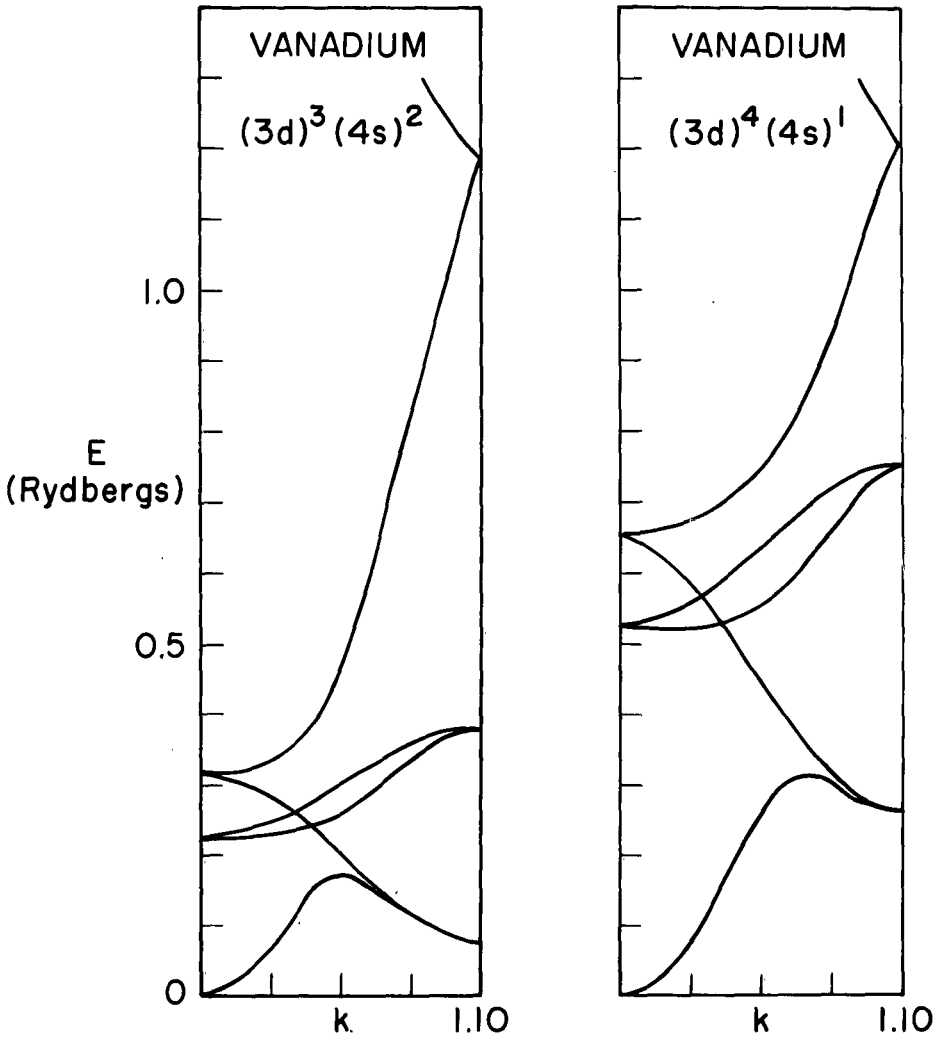

Figure 2

Energy bands for V using potentials obtained from two different atomic configurations. The bands to the left resulted from a configuration of $(3d)^3(4d)^2$, while those to the right involved a $(3d)^4(4s)^1$ configuration.

Similarly, the results for Fe are in good agreement with the published results of Wood[2]. The agreement for A with the results of calculations by Knox and Bassani[16] is good, and has been described previously[5], though there are differences in the ordering of levels. In the case of Cr, it is difficult to compare the present results with those of earlier calculations by Asdente and Friedel[17] since they neglect the interactions between the 3d band and the 4s-4p bands. However, the present results do justify, to some extent, the treatment of Cr by Lomer[18], who used the results of Wood's iron calculations to discuss the energy bands in antiferromagnetic Cr.

In the case of Zn, the ordering of levels is identical with that obtained by Harrison[9]. This ordering differs from that obtained in earlier calculations for hexagonal close packed metals by Herring and Hill for Be[19] and Falicov for Mg[20]. This change in ordering might be due to the presence of an occupied 3d band just below the 4s-4p bands. Finally, the results for Ti agree qualitatively with those obtained by Altmann and Bradley[21].

References

1. J. C. Slater, Phys. Rev. 51, 846 (1937).

2. J. H. Wood, Phys. Rev. 126, 517 (1962).

3. R. E. Watson, Phys. Rev. 119, 1934 (1960) and R. E. Watson and A. J. Freeman, Phys. Rev. 123, 521 (1961).

4. J. C. Slater, Phys. Rev. 81, 385 (1951).

5. L. F. Mattheiss, Quarterly Progress Report Number 46, October 15, 1962, Solid-State and Molecular Theory Group, M.I.T., page 115.

6. P. O. Löwdin, Advances in Physics 5, 1 (1956).

7. W. B. Pearson, A Handbook of Lattice Spacings and Structures of Metals and Alloys, (Pergamon Press, New York, London, Paris, Los Angeles, 1958).

8. E. R. Dobbs and G. O. Jones, Reports on Progress in Physics, edited by A. C. Stickland (The Physical Society, London, 1957), Vol. 20, p. 516.

9. W. A. Harrison, Phys. Rev. 126, 497 (1962).

10. L. P. Bouckaert, R. Smoluchowski, and E. Wigner, Phys. Rev. 50, 58 (1936).

11. C. Herring, J. Franklin Inst. 233, 525 (1942).

12. J. C. Slater, Rev. Mod. Phys. 25, 199 (1953).

13. J. Callaway, Phys. Rev. 99, 500 (1955).

14. B. Segall, Phys. Rev. 125, 109 (1962).

15. G. A. Burdick, Phys. Rev. 129, 138 (1963).

16. R. S. Knox and F. Bassani, Phys. Rev. 124, 652 (1961).

17. M. Asdente and J. Friedel, Phys. Rev. 124, 384 (1961).

18. W. M. Lomer, Proc. Phys. Soc. (London) 80, 489 (1962).

19. C. Herring and A. G. Hill, Phys. Rev. 58, 132 (1940).

20. L. M. Falicov, Phil. Trans. Roy. Soc. A255, 55 (1962).

21. C. J. Bradley, PhD Thesis, Oxford University (1962).

ENERGY BANDS IN GALLIUM

J. H. Wood

The figures shown in the last progress report should be disregarded as they are considerably in error. We now believe that the structure of the 5-6 Fermi surface (which appears to be the important one experimentally) resembles the corresponding free electron surface shown in figure 14(a) of the paper by Reed and Marcus[1]. The main modifications (which are going to be considerable) to that surface are in the regions of the reflection plane perpendecular to the k_a axis (in that figure) -- this is the region in which the free electron surface allows an "exit" from the zone, in the vicinity of the vertices of the hexagon. We are currently concentrating our calculations in that region of k-space in order to ascertain if an exit is still possible in this region.

Some work has also been going into freeing the APW programs from the muffin tin type potential. This type of potential is somewhat restrictive whenever the volume of space outside the muffins becomes a sizeable fraction of the total cell volume. We do not intend to immediately change over to this for the case of gallium, even though some 60 percent of the cell volume is outside the APW spheres and is being represented by a constant value for the potential. It seems worthwhile to push the present calculations to a conclusion to see if they will give us something sensible in the way of a Fermi surface which would be of use to the experimental people.

We also hope to soon begin testing the program for the diamond type structure.

Reference

1. W. A. Reed and J. A. Marcus, Phys. Rev. 126, 1298 (1962)

SYMMETRY PROPERTIES IN THE SPACE GROUP D_{4h}^{14} ($P4_2/mnm$)

John C. Slater

The space group D_{4h}^{14} ($P4_2/mnm$), having the point group D_{4h}, and the primitive tetragonal Bravais lattice, is found in the rutile structure, occurring in TiO_2 and similar compounds. The three fundamental vectors $\vec{t}_1$, $\vec{t}_2$, $\vec{t}_3$ of the primitive unit cell are given by $\vec{t}_1 = a\vec{i}$, $\vec{t}_2 = a\vec{j}$, $\vec{t}_3 = c\vec{k}$, and the vectors $\vec{b}_1$, $\vec{b}_2$, $\vec{b}_3$ of the reciprocal lattice are $\vec{b}_1 = \vec{i}/a$, $\vec{b}_2 = \vec{j}/a$, $\vec{b}_3 = \vec{k}/c$. The Brillouin zone, and the symmetry points in it, are given in Fig. 1. The positions of the atoms in the rutile structure are as follows:

Titanium at the origin of the cell, and at the point for which x/a, y/a, z/c are $1/2, 1/2, 1/2$.

Oxygen at $\pm(uu0;\ u+1/2,\ 1/2-u,\ 1/2)$, where for TiO_2 the parameter u is 0.31.

The 16 operations of the point group D_{4h} are X_0, $X_{\pm1}$, X_2, Y_0, $Y_{\pm1}$, Y_2, X'_0, $X'_{\pm1}$, X'_2, Y'_0, $Y'_{\pm1}$, Y'_2, defined by Eqs. (6) . . . (9), Reference 1. That is, we have

$$
\begin{aligned}
X_q\psi(r,\phi,z) &= \psi\left(r,\phi+\frac{2\pi q}{N},\ z\right)\\
Y_q\psi(r,\phi,z) &= \psi\left(r,-\phi+\frac{2\pi q}{N},\ z\right)\\
X'_q\psi(r,\phi,z) &= \psi\left(r,\phi+\frac{2\pi q}{N},\ -z\right)\\
Y'_q\psi(r,\phi,z) &= \psi\left(r,-\phi+\frac{2\pi q}{N},\ -z\right)
\end{aligned}
\qquad (1)
$$

where N = 4. For the present purpose it is more convenient to express the operations in rectangular coordinates. We then have

$$
\begin{aligned}
X_0\psi(x,y,z) &= \psi(x,y,z) & X'_0\psi(x,y,z) &= \psi(x,y,-z)\\
X_1\psi(x,y,z) &= \psi(-y,x,z) & X'_1\psi(x,y,z) &= \psi(-y,x,-z)\\
X_{-1}\psi(x,y,z) &= \psi(y,-x,z) & X'_{-1}\psi(x,y,z) &= \psi(y,-x,-z)\\
X_2\psi(x,y,z) &= \psi(-x,-y,z) & X'_2\psi(x,y,z) &= \psi(-x,-y,-z)\\
Y_0\psi(x,y,z) &= \psi(x,-y,z) & Y'_0\psi(x,y,z) &= \psi(x,-y,-z)\\
Y_1\psi(x,y,z) &= \psi(y,x,z) & Y'_1\psi(x,y,z) &= \psi(y,x,-z)\\
Y_{-1}\psi(x,y,z) &= \psi(-y,-x,z) & Y'_{-1}\psi(x,y,z) &= \psi(-y,-x,-z)\\
Y_2\psi(x,y,z) &= \psi(-x,y,z) & Y'_2\psi(x,y,z) &= \psi(-x,y,-z)
\end{aligned}
\qquad (2)
$$

The multiplication table for the point group is as given in Eq. (5), Ref. 1, namely

$$X_qX_p = X_{q+p},\ X_qY_p = Y_{-q+p},\ Y_qX_p = Y_{p+q},\ Y_qY_p = X_{-q+p} \qquad (3)$$

In this expression, if the subscript of the product function does not have one of the allowed values 0, ±1, 2, we are to add or subtract integral multiples of 4 to secure a value within this range. In the space group D_{4h}^{14}, we have no non-primitive translation associated with operators with even subscripts, but the non-primitive translation $(\vec{t}_1+\vec{t}_2+\vec{t}_3)/2$ associated with all operators with odd subscripts.

The effect of the operators of Eq. (2) on a plane wave $\exp 2\pi i\,[(h_1+p_1)\xi+(h_2+p_2)\eta+(h_3+p_3)\zeta]$, where the vector position $\vec{r}$ is given by $\xi\vec{t}_1 + \eta\vec{t}_2 + \zeta\vec{t}_3$, is given by Eq. (4) below:

$$
\begin{aligned}
X_0\psi &= \exp 2\pi i\,[(h_1+p_1)\xi+(h_2+p_2)\eta+(h_3+p_3)\zeta]\\
X_1\psi &= \exp 2\pi i\,[(h_2+p_2)\xi-(h_1+p_1)\eta+(h_3+p_3)\zeta]\\
X_{-1}\psi &= \exp 2\pi i\,[-(h_2+p_2)\xi+(h_1+p_1)\eta+(h_3+p_3)\zeta]\\
X_2\psi &= \exp 2\pi i\,[-(h_1+p_1)\xi-(h_2+p_2)\eta+(h_3+p_3)\zeta]\\
Y_0\psi &= \exp 2\pi i\,[(h_1+p_1)\xi-(h_2+p_2)\eta+(h_3+p_3)\zeta]\\
Y_1\psi &= \exp 2\pi i\,[(h_2+p_2)\xi+(h_1+p_1)\eta+(h_3+p_3)\zeta]\\
Y_{-1}\psi &= \exp 2\pi i\,[-(h_2+p_2)\xi-(h_1+p_1)\eta+(h_3+p_3)\zeta]\\
Y_2\psi &= \exp 2\pi i\,[-(h_1+p_1)\xi+(h_2+p_2)\eta+(h_3+p_3)\zeta]
\end{aligned}
\qquad (4)
$$

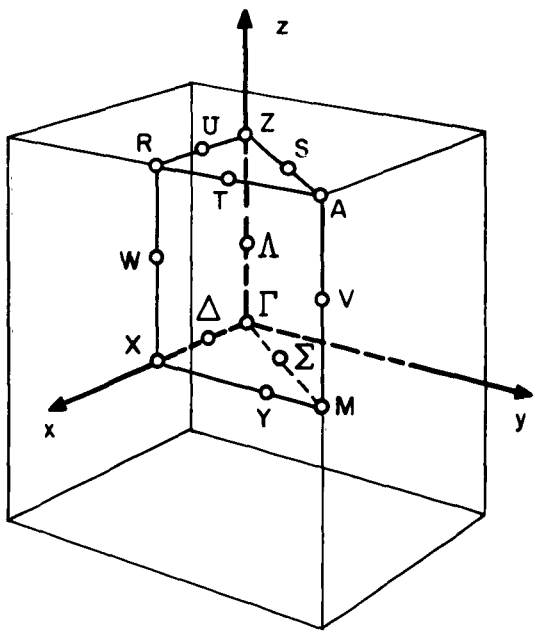

Fig. I Brillouin zone and symmetry points for the primitive tetragonal Bravais lattice

For the primed operations, the sign of h_3+p_3 is to be changed. An additional factor $\exp \pi i(h_1+p_1+h_2+p_2+h_3+p_3)$ occurs for the operations with odd subscripts in the space group, on account of the non-primitive translations. In the multiplication table of the space group, there is an additional factor, arising from the non-primitive translation, if the first operation in the product has an odd subscript. There is no such factor if the first operation has an even subscript. The factor is independent of which odd-subscript operator we have, and is as follows, where we first enumerate the second operation, then the factor:

$$
\begin{array}{ll}
X_0 : 1 & X'_0 : e^{-2\pi i p_3} \\
X_1 : e^{2\pi i(p_2+p_3)} & X'_1 : e^{2\pi i p_2} \\
X_{-1} : e^{2\pi i(p_1+p_3)} & X'_{-1} : e^{2\pi i p_1} \\
X_2 : e^{-2\pi i(p_1+p_2)} & X'_2 : e^{-2\pi i(p_1+p_2+p_3)} \\
Y_0 : e^{-2\pi i p_2} & Y'_0 : e^{-2\pi i(p_2+p_3)} \\
Y_1 : e^{2\pi i(p_1+p_2+p_3)} & Y'_1 : e^{2\pi i(p_1+p_2)} \\
Y_{-1} : e^{2\pi i p_3} & Y'_{-1} : 1 \\
Y_2 : e^{-2\pi i p_1} & Y'_2 : e^{-2\pi i(p_1+p_3)}
\end{array}
\qquad (5)
$$

We now give in Tables 1 . . . 14 the matrix elements and characters for the various symmetry directions, and in Table 15 the compatibility relations.

Table 1

Matrix elements and characters at point Γ, $p_1 = p_2 = p_3 = 0$. Only the matrix elements for the unprimed operators are tabulated. For the primed operators, the elements are the same as for the unprimed for the representations with superscript +, and the negatives of these values for the representations with superscript -.

	X_0	X_1	X_{-1}	X_2	Y_0	Y_1	Y_{-1}	Y_2
$\Gamma_1^{\pm}$	1	1	1	1	1	1	1	1
$\Gamma_2^{\pm}$	1	1	1	1	-1	-1	-1	-1
$\Gamma_3^{\pm}$	1	-1	-1	1	1	-1	-1	1
$\Gamma_4^{\pm}$	1	-1	-1	1	-1	1	1	-1
$(\Gamma_5^{\pm})_{11}$	1	0	0	-1	1	0	0	-1
$(\Gamma_5^{\pm})_{21}$	0	-1	1	0	0	1	-1	0
$(\Gamma_5^{\pm})_{12}$	0	1	-1	0	0	1	-1	0
$(\Gamma_5^{\pm})_{22}$	1	0	0	-1	-1	0	0	1
$\chi(\Gamma_5^{\pm})$	2	0	0	-2	0	0	0	0

Table 2

Matrix elements at points Δ, $p_1 = p$, $p_2 = p_3 = 0$

	X_0	Y_0	X_0'	Y_0'
Δ_1	1	1	1	1
Δ_2	1	-1	-1	1
Δ_3	1	-1	1	-1
Δ_4	1	1	-1	-1

Table 3

Matrix elements at point X, boundary of zone along direction Δ. Here $p_1 = 1/2$, $p_2 = p_3 = 0$.

	X_0	X_2	Y_0	Y_2	X'_0	X'_2	Y'_0	Y'_2
X_1	1	1	1	1	1	1	1	1
X_2	1	-1	1	-1	1	-1	1	-1
X_3	1	-1	-1	1	1	-1	-1	1
X_4	1	1	1	1	-1	-1	-1	-1
X_5	1	-1	-1	1	-1	1	1	-1
X_6	1	-1	1	-1	-1	1	-1	1
X_7	1	1	-1	-1	1	1	-1	-1
X_8	1	1	-1	-1	-1	-1	1	1

Table 4

Matrix elements and characters for points Λ, $p_1 = p_2 = 0$, $p_3 = p$.

	X_0	X_1	X_{-1}	X_2	Y_0	Y_1	Y_{-1}	Y_2
Λ_1	1	$e^{\pi ip}$	$e^{\pi ip}$	1	1	$e^{\pi ip}$	$e^{\pi ip}$	1
Λ_2	1	$e^{\pi ip}$	$e^{\pi ip}$	1	-1	$-e^{\pi ip}$	$-e^{\pi ip}$	-1
Λ_3	1	$-e^{\pi ip}$	$-e^{\pi ip}$	1	1	$-e^{\pi ip}$	$-e^{\pi ip}$	1
Λ_4	1	$-e^{\pi ip}$	$-e^{\pi ip}$	1	-1	$e^{\pi ip}$	$e^{\pi ip}$	-1
$(\Lambda_5)_{11}$	1	0	0	-1	1	0	0	-1
$(\Lambda_5)_{21}$	0	$-e^{\pi ip}$	$e^{\pi ip}$	0	0	$e^{\pi ip}$	$-e^{\pi ip}$	0
$(\Lambda_5)_{12}$	0	$e^{\pi ip}$	$-e^{\pi ip}$	0	0	$e^{\pi ip}$	$-e^{\pi ip}$	0
$(\Lambda_5)_{22}$	1	0	0	-1	-1	0	0	1
$\chi(\Lambda_5)$	2	0	0	-2	0	0	0	0

Table 5

Matrix elements and characters for point Z, boundary of zone along direction Λ. Here $p_1 = p_2 = 0$, $p_3 = 1/2$.

	X_0	X_1	X_{-1}	X_2	Y_0	Y_1	Y_{-1}	Y_2	X'_0	X'_1	X'_{-1}	X'_2	Y'_0	Y'_1	Y'_{-1}	Y'_2
$(Z_1)_{11}$	1	0	0	1	1	0	0	1	0	1	1	0	0	1	1	0
$(Z_1)_{21}$	0	1	1	0	0	1	1	0	1	0	0	1	1	0	0	1
$(Z_1)_{12}$	0	-1	-1	0	0	-1	-1	0	1	0	0	1	1	0	0	1
$(Z_1)_{22}$	1	0	0	1	1	0	0	1	0	-1	-1	0	0	-1	-1	0
$\chi(Z_1)$	2	0	0	2	2	0	0	2	0	0	0	0	0	0	0	0
$(Z_2)_{11}$	1	0	0	1	-1	0	0	-1	0	1	1	0	0	-1	-1	0
$(Z_2)_{21}$	0	1	1	0	0	-1	-1	0	1	0	0	1	-1	0	0	-1
$(Z_2)_{12}$	0	-1	-1	0	0	1	1	0	1	0	0	1	-1	0	0	-1
$(Z_2)_{22}$	1	0	0	1	-1	0	0	-1	0	-1	-1	0	0	1	1	0
$\chi(Z_2)$	2	0	0	2	-2	0	0	-2	0	0	0	0	0	0	0	0
$(Z_3)_{11}$	1	0	0	-1	1	0	0	-1	1	0	0	-1	1	0	0	-1
$(Z_3)_{21}$	0	1	-1	0	0	-1	1	0	0	-1	1	0	0	1	-1	0
$(Z_3)_{12}$	0	1	-1	0	0	1	-1	0	0	1	-1	0	0	1	-1	0
$(Z_3)_{22}$	1	0	0	-1	-1	0	0	1	-1	0	0	1	1	0	0	-1
$\chi(Z_3)$	2	0	0	-2	0	0	0	0	0	0	0	0	2	0	0	-2
$(Z_4)_{11}$	1	0	0	-1	1	0	0	-1	-1	0	0	1	-1	0	0	1
$(Z_4)_{21}$	0	1	-1	0	0	-1	1	0	0	1	-1	0	0	-1	1	0
$(Z_4)_{12}$	0	1	-1	0	0	1	1	0	0	-1	1	0	0	-1	1	0
$(Z_4)_{22}$	1	0	0	-1	-1	0	0	1	1	0	0	-1	-1	0	0	1
$\chi(Z_4)$	2	0	0	-2	0	0	0	0	0	0	0	0	-2	0	0	2

Table 6

Matrix elements for points Σ, $p_1 = p_2 = p$, $p_3 = 0$

	X_0	Y_1	X_0'	Y_1'
Σ_1	1	$e^{2\pi ip}$	1	$e^{2\pi ip}$
Σ_2	1	$-e^{2\pi ip}$	-1	$e^{2\pi ip}$
Σ_3	1	$e^{2\pi ip}$	-1	$-e^{2\pi ip}$
Σ_4	1	$-e^{2\pi ip}$	1	$-e^{2\pi ip}$

Table 7

Matrix elements and characters for point M, boundary of zone along direction Σ. Here $p_1 = p_2 = 1/2$, $p_3 = 0$. In the table below the matrix elements for the primed operations are equal to those for the unprimed for superscript +, and the negative of these values for superscript - .

	X_0	X_1	X_{-1}	X_2	Y_0	Y_1	Y_{-1}	Y_2
$M_1^{\pm}$	1	1	-1	-1	1	1	-1	-1
$M_2^{\pm}$	1	1	-1	-1	-1	-1	1	1
$M_3^{\pm}$	1	-1	1	-1	1	-1	1	-1
$M_4^{\pm}$	1	-1	1	-1	-1	1	-1	1
$(M_5^{\pm})_{11}$	1	0	0	1	0	1	1	0
$(M_5^{\pm})_{21}$	0	1	1	0	1	0	0	1
$(M_5^{\pm})_{12}$	0	-1	-1	0	1	0	0	1
$(M_5^{\pm})_{22}$	1	0	0	1	0	-1	-1	0
$\chi(M_5^{\pm})$	2	0	0	2	0	0	0	0

Table 8

Matrix elements for directions W, $p_1 = 1/2$, $p_2 = 0$, $p_3 = p$. For point X, $p = 0$. For point R, $p = 1/2$.

	X_0	X_2	Y_0	Y_2
W_1	1	1	1	1
W_2	1	1	-1	-1
W_3	1	-1	1	-1
W_4	1	-1	-1	1

Table 9

Matrix elements for direction R, $p_1 = p_3 = 1/2$, $p_2 = 0$

	X_0	X_2	Y_0	Y_2	X_0'	X_2'	Y_0'	Y_2'
R_1	1	1	1	1	1	1	1	1
R_2	1	-1	1	-1	1	-1	1	-1
R_3	1	-1	-1	1	1	-1	-1	1
R_4	1	1	1	1	-1	-1	-1	-1
R_5	1	-1	-1	1	-1	1	1	-1
R_6	1	-1	1	-1	-1	1	-1	1
R_7	1	1	-1	-1	1	1	-1	-1
R_8	1	1	-1	-1	-1	-1	1	1

Table 10

Matrix elements and characters at points V, joining M and A. Here $p_1 = p_2 = 1/2$, $p_3 = p$. At M, $p = 0$; at A, $p = 1/2$.

	X_0	X_1	X_{-1}	X_2	Y_0	Y_1	Y_{-1}	Y_2
V_1	1	$e^{\pi ip}$	$-e^{\pi ip}$	-1	1	$e^{\pi ip}$	$-e^{\pi ip}$	-1
V_2	1	$e^{\pi ip}$	$-e^{\pi ip}$	-1	-1	$-e^{\pi ip}$	$e^{\pi ip}$	1
V_3	1	$-e^{\pi ip}$	$e^{\pi ip}$	-1	1	$-e^{\pi ip}$	$e^{\pi ip}$	-1
V_4	1	$-e^{\pi ip}$	$e^{\pi ip}$	-1	-1	$e^{\pi ip}$	$-e^{\pi ip}$	1
$(V_5)_{11}$	1	0	0	1	1	0	0	1
$(V_5)_{21}$	0	$e^{\pi ip}$	$e^{\pi ip}$	0	0	$-e^{\pi ip}$	$-e^{\pi ip}$	0
$(V_5)_{12}$	0	$-e^{\pi ip}$	$-e^{\pi ip}$	0	0	$-e^{\pi ip}$	$-e^{\pi ip}$	0
$(V_5)_{22}$	1	0	0	1	-1	0	0	-1
$\chi(V_5)$	2	0	0	2	0	0	0	0

Table 11

Matrix elements and characters for point A, $p_1 = p_2 = p_3 = 1/2$

	X_0	X_1	X_{-1}	X_2	Y_0	Y_1	Y_{-1}	Y_2	X'_0	X'_1	X'_{-1}	X'_2	Y'_0	Y'_1	Y'_{-1}	Y'_2
$(A_1)_{11}$	1	1	1	1	0	0	0	0	0	0	0	0	1	1	1	1
$(A_1)_{21}$	0	0	0	0	1	1	1	1	1	1	1	1	0	0	0	0
$(A_1)_{12}$	0	0	0	0	1	-1	-1	1	1	-1	-1	1	0	0	0	0
$(A_1)_{22}$	1	-1	-1	1	0	0	0	0	0	0	0	0	1	-1	-1	1
$\chi(A_1)$	2	0	0	2	0	0	0	0	0	0	0	0	2	0	0	2
$(A_2)_{11}$	1	1	1	1	0	0	0	0	0	0	0	0	-1	-1	-1	-1
$(A_2)_{21}$	0	0	0	0	1	1	1	1	-1	-1	-1	-1	0	0	0	0
$(A_2)_{12}$	0	0	0	0	1	-1	-1	1	-1	1	1	-1	0	0	0	0
$(A_2)_{22}$	1	-1	-1	1	0	0	0	0	0	0	0	0	-1	1	1	-1
$\chi(A_2)$	2	0	0	2	0	0	0	0	0	0	0	0	-2	0	0	-2
$(A_3)_{11}$	1	0	0	-1	1	0	0	-1	1	0	0	-1	1	0	0	-1
$(A_3)_{21}$	0	1	-1	0	0	1	-1	0	0	-1	1	0	0	-1	1	0
$(A_3)_{12}$	0	-1	1	0	0	-1	1	0	0	-1	1	0	0	-1	1	0
$(A_3)_{22}$	1	0	0	-1	1	0	0	-1	-1	0	0	1	-1	0	0	1
$\chi(A_3)$	2	0	0	-2	2	0	0	-2	0	0	0	0	0	0	0	0
$(A_4)_{11}$	1	0	0	-1	-1	0	0	1	-1	0	0	1	1	0	0	-1
$(A_4)_{21}$	0	1	-1	0	0	-1	1	0	0	1	-1	0	0	-1	1	0
$(A_4)_{12}$	0	-1	1	0	0	1	-1	0	0	1	-1	0	0	-1	1	0
$(A_4)_{22}$	1	0	0	-1	-1	0	0	1	1	0	0	-1	-1	0	0	1
$\chi(A_4)$	2	0	0	-2	-2	0	0	2	0	0	0	0	0	0	0	0

Table 12

Matrix elements at points U, connecting Z and R. Here $p_1 = p$, $p_2 = 0$, $p_3 = 1/2$. At Z, $p = 0$; at R, $p = 1/2$.

	X_0	Y_0	X_0'	Y_0'
U_1	1	1	1	1
U_2	1	-1	-1	1
U_3	1	-1	1	-1
U_4	1	1	-1	-1

Table 13

Matrix elements at points T, connecting R and A. Here $p_1 = p_3 = 1/2$, $p_2 = p$. At R, $p = 0$; at A, $p = 1/2$.

	X_0	Y_2	X_0'	Y_2'
T_1	1	1	1	1
T_2	1	-1	-1	1
T_3	1	-1	1	-1
T_4	1	1	-1	-1

Table 14

Matrix elements and characters at points S, connecting Z and A. Here $p_1 = p_2 = p$, $p_3 = 1/2$. At Z, $p = 0$; at A, $p = 1/2$.

	X_0	Y_1	X_0'	Y_1'
$(S_1)_{11}$	1	0	1	0
$(S_1)_{21}$	0	$e^{2\pi ip}$	0	$-e^{2\pi ip}$
$(S_1)_{12}$	0	$-e^{2\pi ip}$	0	$-e^{2\pi ip}$
$(S_1)_{22}$	1	0	-1	0
$\chi(S_1)$	2	0	0	0

Table 15

Compatibility relations

Γ_1^+	Γ_1^-	Γ_2^+	Γ_2^-	Γ_3^+	Γ_3^-	Γ_4^+	Γ_4^-	Γ_5^+	Γ_5^-
Δ_1	Δ_4	Δ_3	Δ_2	Δ_1	Δ_4	Δ_3	Δ_2	$\Delta_1\Delta_3$	$\Delta_2\Delta_4$
Λ_1	Λ_1	Λ_2	Λ_2	Λ_3	Λ_3	Λ_4	Λ_4	Λ_5	Λ_5
Σ_1	Σ_3	Σ_4	Σ_2	Σ_4	Σ_2	Σ_1	Σ_3	$\Sigma_1\Sigma_4$	$\Sigma_2\Sigma_3$

X_1	X_2	X_3	X_4	X_5	X_6	X_7	X_8
Δ_1	Δ_1	Δ_3	Δ_4	Δ_2	Δ_4	Δ_3	Δ_2
Y_1	Y_3	Y_1	Y_4	Y_4	Y_2	Y_3	Y_2
W_1	W_3	W_4	W_1	W_4	W_3	W_2	W_2

Z_1	Z_2	Z_3	Z_4
$\Lambda_1\Lambda_3$	$\Lambda_2\Lambda_4$	Λ_5	Λ_5
U_1U_4	U_2U_3	U_1U_2	U_3U_4
S_1	S_1	S_1	S_1

M_1^+	M_1^-	M_2^+	M_2^-	M_3^+	M_3^-	M_4^+	M_4^-	M_5^+	M_5^-
Σ_4	Σ_2	Σ_1	Σ_3	Σ_1	Σ_3	Σ_4	Σ_2	$\Sigma_1\Sigma_4$	$\Sigma_2\Sigma_3$
Y_3	Y_2	Y_1	Y_4	Y_3	Y_2	Y_1	Y_4	Y_1Y_3	Y_2Y_4
V_1	V_1	V_2	V_2	V_3	V_3	V_4	V_4	V_5	V_5

R_1	R_2	R_3	R_4	R_5	R_6	R_7	R_8
U_1	U_1	U_3	U_4	U_2	U_4	U_3	U_2
W_1	W_3	W_4	W_1	W_4	W_3	W_2	W_2
T_1	T_3	T_1	T_4	T_4	T_2	T_3	T_2

Table 15 (continued)

A_1	A_2	A_3	A_4
S_1	S_1	S_1	S_1
T_1T_2	T_3T_4	T_2T_3	T_1T_4
V_5	V_5	V_1V_3	V_2V_4

References

1. J. C. Slater, Symmetry Properties in the Space Groups D_{6h}^4 and C_{6v}^4, Quarterly Progress Report No. 46, Solid-State and Molecular Theory Group, M.I.T., October 15, 1962, p. 67.

SYMMETRY PROPERTIES IN THE SPACE GROUPS $C_{3i}^2(R\bar{3})$, $D_3^7(R32)$, $D_{3d}^5(R\bar{3}m)$, AND $D_{3d}^6(R\bar{3}c)$

John C. Slater

The space groups considered here have the rhombohedral or trigonal Bravais lattice, and can be conveniently considered together. A good many important elements and compounds crystallize in one or another of these space groups. Thus the ilmenite structure has the space group $C_{3i}^2(R\bar{3})$, the AlF_3 structure has $D_3^7(R32)$, the arsenic structure, the $CdCl_2$ structure, and the LaOF structure have the space group $D_{3d}^5(R\bar{3}m)$, and the calcite and corundum structures have the space group $D_{3d}^6(R\bar{3}c)$. Positions of atoms in the structures listed above are given in Table 1.

The three fundamental vectors $\vec{t}_1$, $\vec{t}_2$, $\vec{t}_3$ of the primitive unit cell are of equal magnitude, and make equal angles of α with each other. In rectangular coordinates they are expressed as

$$\vec{t}_1 = s\vec{i} + r\vec{k},\ \vec{t}_2 = \frac{s}{2}(-\vec{i} + \sqrt{3}\vec{j}) + r\vec{k},\ \vec{t}_3 = \frac{s}{2}(-\vec{i} - \sqrt{3}\vec{j}) + r\vec{k} \qquad (1)$$

The length of the vectors $\vec{t}_1$, $\vec{t}_2$, $\vec{t}_3$ is $\sqrt{s^2+r^2}$, and the angle α is given by the equation

$$\cos\alpha = \frac{-s^2/2 + r^2}{s^2+r^2} \qquad (2)$$

from which we can find s and r when the length of the vector and the angle α are given, as is usual in crystallographic work. The vectors $\vec{b}_1$, $\vec{b}_2$, $\vec{b}_3$ of the reciprocal lattice are given by

$$\vec{b}_1 = s'\vec{i} + r'\vec{k},\ \vec{b}_2 = \frac{s'}{2}(-\vec{i} + \sqrt{3}\vec{j}) + r'\vec{k},\ \vec{b}_3 = \frac{s'}{2}(-\vec{i} - \sqrt{3}\vec{j}) + r'\vec{k} \qquad (3)$$

where $$s' = 2/3s, \quad r' = 1/3r \tag{4}$$

From Eq. (3) we see that the reciprocal lattice is also rhombohedral. The Brillouin zone is shown in Fig. 1, with convenient notations (partly following Koster[1]) for the symmetry directions. The inclined hexagonal faces are perpendicular bisectors of vectors $\pm\vec{b}_1$, $\pm\vec{b}_2$, $\pm\vec{b}_3$. The rectangular faces are perpendicular bisectors of the vectors $\pm(\vec{b}_1+\vec{b}_2)$, $\pm(\vec{b}_2+\vec{b}_3)$, $\pm(\vec{b}_1+\vec{b}_3)$, and the top and bottom faces are perpenticular bisectors of the vectors $\pm(\vec{b}_1+\vec{b}_2+\vec{b}_3)$. The height of the Brillouin zone is $3r'$, and the dividing lines between the rectangular faces and the inclined hexagonal faces come at distances r' and $2r'$ from the top and bottom faces. The symmetry points indicated by A and B in Fig. 1 are the intersections of the vectors $\pm\vec{b}_1$, etc., and $\pm(\vec{b}_1+\vec{b}_2)$, etc., with the faces of the Brillouin zone.

The point groups C_{3i} and D_3, which are found in the first two space groups considered, may be taken as special cases of D_{3d}, met with the remaining two. Consequently we shall carry through the case of D_{3d}, and shall specialize for the other cases. The operations of the point group D_{3d}, in cylindrical coordinates, may be taken to be defined by

$$\begin{aligned}
X_0\psi(r,\phi,z) &= \psi(r,\phi,z)\\
X_{\pm1}\psi(r,\phi,z) &= \psi(r,\phi\pm\tfrac{\pi}{3},-z)\\
X_{\pm2}\psi(r,\phi,z) &= \psi(r,\phi\pm\tfrac{2\pi}{3},z)\\
X_3\psi\ (r,\phi,z) &= \psi(r,\phi+\pi,-z)\\
Y_0\psi(r,\phi,z) &= \psi(r,-\phi,z)\\
Y_{\pm1}\psi(r,\phi,z) &= \psi(r,-\phi\pm\tfrac{\pi}{3},-z)\\
Y_{\pm2}\psi(r,\phi,z) &= \psi(r,-\phi\pm\tfrac{2\pi}{3},z)\\
Y_3\psi\ (r,\phi,z) &= \psi(r,-\phi+\pi,-z)
\end{aligned} \tag{5}$$

The operations of C_{3i} may be described in terms of Eq. (5) as the X operations listed there; the operations of D_3 may be described as X_0, $X_{\pm2}$, $Y_{\pm1}$, Y_3. In Table 2 we describe the operations of D_{3d} in terms of their effect on a function of the vector $\vec{r}$ expressed in the form

$$\vec{r} = \xi\vec{t}_1 + \eta\vec{t}_2 + \zeta\vec{t}_3 \tag{6}$$

In Table 3 we show the effect of these operations on a plane wave of the form

$$\psi = \exp 2\pi i[\,(h_1+p_1)\vec{b}_1+(h_2+p_2)\vec{b}_2+(h_3+p_3)\vec{b}_3\,]\cdot\vec{r} \tag{7}$$

where the reduced wave vector is $2\pi(p_1\vec{b}_1+p_2\vec{b}_2+p_3\vec{b}_3)$, and the h's are integers. These operations combine according to the multiplication table

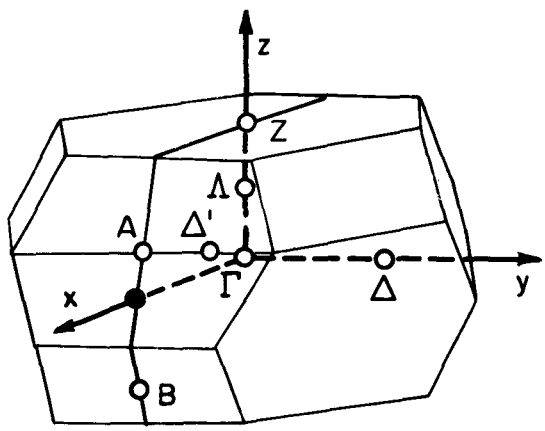

Fig. 1 Brillouin zone for the rhombohedral Bravais lattice, with notation for symmetry directions.

$$\begin{aligned} X_q X_p &= X_{q+p} \\ X_q Y_p &= Y_{-q+p} \\ Y_p X_q &= Y_{p+q} \\ Y_q Y_p &= X_{-q+p} \end{aligned} \tag{7}$$

in which if any subscript lies outside the range from -2 to 3, we are to add or subtract integral multiples of 6 to bring it within this range.

The space groups under consideration are symmorphic, except for the case of $D_{3d}^6(R\bar{3}c)$. Consequently the multiplication table as just stated can be used for the space groups as well as for the point groups. For the case of $D_{3d}^6(R\bar{3}c)$, a non-primitive translation $(1/2)(\vec{t}_1+\vec{t}_2+\vec{t}_3)$ is associated with each of the Y operations; no non-primitive translation is associated with the X's. Consequently the effect of one of the Y operations on a plane wave is found from Table 3 by multiplying the value given by that table by the factor

$$e^{\pi i(h_1+p_1+h_2+p_2+h_3+p_3)} \tag{8}$$

The effect of these non-primitive translations on the multiplication table for the space group $D_{3d}^6(R\bar{3}c)$ is found by using Eq. (7), and multiplying the result by an extra factor as follows:

Any Y operating on an X with an odd subscript,
factor $e^{-2\pi i(p_1+p_2+p_3)}$

Any Y operating on a Y with an even subscript,
factor $e^{2\pi i(p_1+p_2+p_3)}$ (9)

In all other cases there is no extra factor.

We now give in the remaining tables the matrix elements for the various irreducible representations of the four space groups under consideration, and the compatibility relations. Since there is no generally accepted convention for the naming of the irreducible representations of these space groups, we have introduced names for them.

Table 1

Positions of Atoms in Structures Having Space Groups Under Discussion

Ilmenite Structure C_{3i}^2 ($R\bar{3}$). $FeTiO_3$. Iron atoms at positions $\xi = u$, $\eta = u$, $\zeta = u$ and $\xi = -u$, $\eta = -u$, $\zeta = -u$, where $u = 0.358$; titanium atoms for $\xi = v$, $\eta = v$, $\zeta = v$, and $\xi = -v$, $\eta = -v$, $\zeta = -v$, where $v = 0.142$; and oxygens at general positions $\pm(\xi\eta\zeta, \eta\zeta\xi, \zeta\xi\eta)$, where $\xi = 0.555$, $\eta = -0.055$, and $\zeta = 0.250$. Other similar compounds have similar parameters.

AlF_3 Structure D_3^7(R32). Aluminum atoms at uuu and $\bar{u}\bar{u}\bar{u}$ (that is, $\xi = u$, $\eta = u$, $\zeta = u$ and $\xi = -u$, $\eta = -u$, $\zeta = -u$) where $u = 0.237$. One type of fluorine at $0v\bar{v}$, $\bar{v}0v$, $v\bar{v}0$, where $v = 0.430$. Another type of fluorine at $1/2, w\bar{w}; \bar{w}, 1/2, w; w\bar{w}, 1/2$, where $w = 0.070$. Other similar compounds have similar parameters.

Arsenic Structure D_{3d}^5 ($R\bar{3}m$). Arsenic atoms at uuu and $\bar{u}\bar{u}\bar{u}$, where $u = 0.226$ for arsenic.

$CdCl_2$ Structure D_{3d}^5 ($R\bar{3}m$). Cadmium atom at origin, chlorine atoms at uuu and $\bar{u}\bar{u}\bar{u}$, where u is approximately $1/4$.

LaOF Structure D_{3d}^5 ($R\bar{3}m$). Lanthanum atoms at uuu, $\bar{u}\bar{u}\bar{u}$, where $u = 0.242$. Fluorines in similar positions with $u = 0.122$; oxygens in similar positions, with $u = 0.370$.

Calcite Structure D_{3d}^6 ($R\bar{3}c$) $CaCO_3$. Calcium atoms at origin, and $1/2, 1/2, 1/2$. Carbons at $\pm(1/4, 1/4, 1/4)$. Oxygens at $\pm(1/4-u, 1/4+u, 1/4)$; $1/4+u, 1/4, 1/4-u; 1/4, 1/4-u, 1/4+u)$, where $u = 0.243$.

Corundum Structure D_{3d}^6 ($R\bar{3}c$) Al_2O_3. Aluminum atoms at $\pm(1/4+u, 1/4+u, 1/4+u; 1/4-u, 1/4-u, 1/4-u)$, with $u = 0.105$. Oxygens at $\pm(1/4-v, 1/4+v, 1/4; 1/4+v, 1/4, 1/4-v; 1/4, 1/4-v, 1/4+v)$, with $v = 0.303$.

Table 2

Operations of the Point Group D_{3d}

$$X_0\psi(\vec{r}) = \psi(\xi\vec{t}_1+\eta\vec{t}_2+\zeta\vec{t}_3)$$
$$X_1\psi(\vec{r}) = \psi(-\eta\vec{t}_1-\zeta\vec{t}_2-\xi\vec{t}_3)$$
$$X_{-1}\psi(\vec{r}) = \psi(-\zeta\vec{t}_1-\xi\vec{t}_2-\eta\vec{t}_3)$$
$$X_2\psi(\vec{r}) = \psi(\zeta\vec{t}_1+\xi\vec{t}_2+\eta\vec{t}_3)$$
$$X_{-2}\psi(\vec{r}) = \psi(\eta\vec{t}_1+\zeta\vec{t}_2+\xi\vec{t}_3)$$
$$X_3\psi(\vec{r}) = \psi(-\xi\vec{t}_1-\eta\vec{t}_2-\zeta\vec{t}_3)$$
$$Y_0\psi(\vec{r}) = \psi(\xi\vec{t}_1+\zeta\vec{t}_2+\eta\vec{t}_3)$$
$$Y_1\psi(\vec{r}) = \psi(-\zeta\vec{t}_1-\eta\vec{t}_2-\xi\vec{t}_3)$$
$$Y_{-1}\psi(\vec{r}) = \psi(-\eta\vec{t}_1-\xi\vec{t}_2-\zeta\vec{t}_3)$$
$$Y_2\psi(\vec{r}) = \psi(\eta\vec{t}_1+\xi\vec{t}_2+\zeta\vec{t}_3)$$
$$Y_{-2}\psi(\vec{r}) = \psi(\zeta\vec{t}_1+\eta\vec{t}_2+\xi\vec{t}_3)$$
$$Y_3\psi(\vec{r}) = \psi(-\xi\vec{t}_1-\zeta\vec{t}_2-\eta\vec{t}_3)$$

Table 3

Effect of Operators of D_{3d} on a Plane Wave

$$X_0\psi = \exp 2\pi i\,[(h_1+p_1)\xi+(h_2+p_2)\eta+(h_3+p_3)\zeta]$$
$$X_1\psi = \exp 2\pi i\,[-(h_3+p_3)\xi-(h_1+p_1)\eta-(h_2+p_2)\zeta]$$
$$X_{-1}\psi = \exp 2\pi i\,[-(h_2+p_2)\xi-(h_3+p_3)\eta-(h_1+p_1)\zeta]$$
$$X_2\psi = \exp 2\pi i\,[(h_2+p_2)\xi+(h_3+p_3)\eta+(h_1+p_1)\zeta]$$
$$X_{-2}\psi = \exp 2\pi i\,[(h_3+p_3)\xi+(h_1+p_1)\eta+(h_2+p_2)\zeta]$$
$$X_3\psi = \exp 2\pi i\,[-(h_1+p_1)\xi-(h_2+p_2)\eta-(h_3+p_3)\zeta]$$
$$Y_0\psi = \exp 2\pi i\,[(h_1+p_1)\xi+(h_3+p_3)\eta+(h_2+p_2)\zeta]$$
$$Y_1\psi = \exp 2\pi i\,[-(h_3+p_3)\xi-(h_2+p_2)\eta-(h_1+p_1)\zeta]$$
$$Y_{-1}\psi = \exp 2\pi i\,[-(h_2+p_2)\xi-(h_1+p_1)\eta-(h_3+p_3)\zeta]$$
$$Y_2\psi = \exp 2\pi i\,[(h_2+p_2)\xi+(h_1+p_1)\eta+(h_3+p_3)\zeta]$$
$$Y_{-2}\psi = \exp 2\pi i\,[(h_3+p_3)\xi+(h_2+p_2)\eta+(h_1+p_1)\zeta]$$
$$Y_3\psi = \exp 2\pi i\,[-(h_1+p_1)\xi-(h_3+p_3)\eta-(h_2+p_2)\zeta]$$

Table 4

Matrix elements and characters at point Γ. $p_1 = p_2 = p_3 = 0$. The abbreviation ω stands for $e^{2\pi i/3}$.

C_{3i}^2 $(R\bar{3})$

	X_0	X_1	X_{-1}	X_2	X_{-2}	X_3
Γ_1	1	1	1	1	1	1
Γ_2	1	ω	ω^2	ω^2	ω	1
Γ_3	1	ω^2	ω	ω	ω^2	1
Γ_4	1	$-\omega^2$	$-\omega$	ω	ω^2	-1
Γ_5	1	$-\omega$	$-\omega^2$	ω^2	ω	-1
Γ_6	1	-1	-1	1	1	-1

D_3^7 (R32)

	X_0	X_2	X_{-2}	Y_1	Y_{-1}	Y_3
Γ_1	1	1	1	1	1	1
Γ_2	1	1	1	-1	-1	-1
$(\Gamma_3)_{11}$	1	ω	ω^2	0	0	0
$(\Gamma_3)_{21}$	0	0	0	ω^2	ω	1
$(\Gamma_3)_{12}$	0	0	0	ω	ω^2	1
$(\Gamma_3)_{22}$	1	ω^2	ω	0	0	0
$\chi(\Gamma_3)$	2	-1	-1	0	0	0

Table 4 (Continued)

D_{3d}^5 ($R\bar{3}m$) and D_{3d}^6 ($R\bar{3}c$)

	X_0	X_1	X_{-1}	X_2	X_{-2}	X_3	Y_0	Y_1	Y_{-1}	Y_2	Y_{-2}	Y_3
Γ_1	1	1	1	1	1	1	1	1	1	1	1	1
Γ_2	1	1	1	1	1	1	-1	-1	-1	-1	-1	-1
Γ_3	1	-1	-1	1	1	-1	1	-1	-1	1	1	-1
Γ_4	1	-1	-1	1	1	-1	-1	1	1	-1	-1	1
$(\Gamma_5)_{11}$	1	$-\frac{1}{2}$	$-\frac{1}{2}$	$-\frac{1}{2}$	$-\frac{1}{2}$	1	1	$-\frac{1}{2}$	$-\frac{1}{2}$	$-\frac{1}{2}$	$-\frac{1}{2}$	1
$(\Gamma_5)_{21}$	0	$-\frac{\sqrt{3}}{2}$	$\frac{\sqrt{3}}{2}$	$\frac{\sqrt{3}}{2}$	$-\frac{\sqrt{3}}{2}$	0	0	$\frac{\sqrt{3}}{2}$	$-\frac{\sqrt{3}}{2}$	$-\frac{\sqrt{3}}{2}$	$\frac{\sqrt{3}}{2}$	0
$(\Gamma_5)_{12}$	0	$\frac{\sqrt{3}}{2}$	$-\frac{\sqrt{3}}{2}$	$-\frac{\sqrt{3}}{2}$	$\frac{\sqrt{3}}{2}$	0	0	$\frac{\sqrt{3}}{2}$	$-\frac{\sqrt{3}}{2}$	$-\frac{\sqrt{3}}{2}$	$\frac{\sqrt{3}}{2}$	0
$(\Gamma_5)_{22}$	1	$-\frac{1}{2}$	$-\frac{1}{2}$	$-\frac{1}{2}$	$-\frac{1}{2}$	1	-1	$\frac{1}{2}$	$\frac{1}{2}$	$\frac{1}{2}$	$\frac{1}{2}$	-1
$\chi(\Gamma_5)$	2	-1	-1	-1	-1	2	0	0	0	0	0	0
$(\Gamma_6)_{11}$	1	$\frac{1}{2}$	$\frac{1}{2}$	$-\frac{1}{2}$	$-\frac{1}{2}$	-1	1	$\frac{1}{2}$	$\frac{1}{2}$	$-\frac{1}{2}$	$-\frac{1}{2}$	-1
$(\Gamma_6)_{21}$	0	$-\frac{\sqrt{3}}{2}$	$\frac{\sqrt{3}}{2}$	$-\frac{\sqrt{3}}{2}$	$\frac{\sqrt{3}}{2}$	0	0	$\frac{\sqrt{3}}{2}$	$-\frac{\sqrt{3}}{2}$	$\frac{\sqrt{3}}{2}$	$-\frac{\sqrt{3}}{2}$	0
$(\Gamma_6)_{12}$	0	$\frac{\sqrt{3}}{2}$	$-\frac{\sqrt{3}}{2}$	$\frac{\sqrt{3}}{2}$	$-\frac{\sqrt{3}}{2}$	0	0	$\frac{\sqrt{3}}{2}$	$-\frac{\sqrt{3}}{2}$	$\frac{\sqrt{3}}{2}$	$-\frac{\sqrt{3}}{2}$	0
$(\Gamma_6)_{22}$	1	$\frac{1}{2}$	$\frac{1}{2}$	$-\frac{1}{2}$	$-\frac{1}{2}$	-1	-1	$-\frac{1}{2}$	$-\frac{1}{2}$	$\frac{1}{2}$	$\frac{1}{2}$	1
$\chi(\Gamma_6)$	2	1	1	-1	-1	-2	0	0	0	0	0	0

Table 5

Matrix elements and characters for propagation along Λ, z axis. Here $p_1 = p_2 = p_3$. At Γ, p's equal zero. At Z, $p_1 = p_2 = p_3 = 1/2$. Abbreviation ω stands for $e^{2\pi i/3}$.

$\underline{C_{3i}^2\ (R\bar{3})}$ and $\underline{D_3^7\ (R32)}$

	X_0	X_2	X_{-2}
Λ_1	1	1	1
Λ_2	1	ω	ω^2
Λ_3	1	ω^2	ω

$\underline{D_{3d}^5\ (R\bar{3}m)}$ and $\underline{D_{3d}^6\ (R\bar{3}c)}$ The Abbreviation a stands for $e^{\pi i(p_1+p_2+p_3)}$. For the group D_{3d}^5 (R3m) a is to be replaced by unity.

	X_0	X_2	X_{-2}	Y_0	Y_2	Y_{-2}
Λ_1	1	1	1	a	a	a
Λ_2	1	1	1	-a	-a	-a
$(\Lambda_3)_{11}$	1	$-\frac{1}{2}$	$-\frac{1}{2}$	a	$-\frac{a}{2}$	$-\frac{a}{2}$
$(\Lambda_3)_{21}$	0	$\frac{\sqrt{3}}{2}$	$-\frac{\sqrt{3}}{2}$	0	$-\frac{a\sqrt{3}}{2}$	$\frac{a\sqrt{3}}{2}$
$(\Lambda_3)_{12}$	0	$-\frac{\sqrt{3}}{2}$	$\frac{\sqrt{3}}{2}$	0	$-\frac{a\sqrt{3}}{2}$	$\frac{a\sqrt{3}}{2}$
$(\Lambda_3)_{22}$	1	$-\frac{1}{2}$	$-\frac{1}{2}$	-a	$\frac{a}{2}$	$\frac{a}{2}$
$\chi(\Lambda_3)$	2	-1	-1	0	0	0

Table 6

Matrix elements and characters for point Z, $p_1 = p_2 = p_3 = 1/2$. For C_{3i}^2 ($R\bar{3}$), D_3^7 (R32), and D_{3d}^5 ($R\bar{3}m$), the symmetry is identical with Γ, and the same table can be used, replacing the symbols Γ for the representations by Z. The abbreviation ω stands for $e^{2\pi i/3}$.

D_{3d}^6 ($R\bar{3}c$)

	X_0	X_1	X_{-1}	X_2	X_{-2}	X_3	Y_0	Y_1	Y_{-1}	Y_2	Y_{-2}	Y_3
$(Z_1)_{11}$	1	0	0	1	1	0	1	0	0	1	1	0
$(Z_1)_{21}$	0	1	1	0	0	1	0	1	1	0	0	1
$(Z_1)_{12}$	0	1	1	0	0	1	0	-1	-1	0	0	-1
$(Z_1)_{22}$	1	0	0	1	1	0	-1	0	0	-1	-1	0
$\chi(Z_1)$	2	0	0	2	2	0	0	0	0	0	0	0
$(Z_2)_{11}$	1	ω	ω^2	ω^2	ω	1	0	0	0	0	0	0
$(Z_2)_{21}$	0	0	0	0	0	0	1	$-\omega$	$-\omega^2$	ω^2	ω	-1
$(Z_2)_{12}$	0	0	0	0	0	0	-1	$-\omega^2$	$-\omega$	$-\omega$	$-\omega^2$	-1
$(Z_2)_{22}$	1	$-\omega^2$	$-\omega$	ω	ω^2	-1	0	0	0	0	0	0
$\chi(Z_2)$	2	$i\sqrt{3}$	$-i\sqrt{3}$	-1	-1	0	0	0	0	0	0	0
$(Z_3)_{11}$	1	ω^2	ω	ω	ω^2	1	0	0	0	0	0	0
$(Z_3)_{21}$	0	0	0	0	0	0	1	$-\omega^2$	$-\omega$	ω	ω^2	-1
$(Z_3)_{12}$	0	0	0	0	0	0	-1	$-\omega$	$-\omega^2$	$-\omega^2$	$-\omega$	-1
$(Z_3)_{22}$	1	$-\omega$	$-\omega^2$	ω^2	ω	-1	0	0	0	0	0	0
$\chi(Z_3)$	2	$-i\sqrt{3}$	$-\sqrt{3}$	-1	-1	0	0	0	0	0	0	0

Table 7

Matrix elements and characters for propagation along **Δ**, y axis, and **Δ'**, direction parallel to y axis passing through A. For the group C_{3i}^2 ($R\bar{3}$) these are not symmetry directions. For **Δ**, $p_1 = 0$, $p_2 = -p_3$. For **Δ'**, $p_1 = 1/2$, $p_2 = -p_3$. Point A, $p_1 = 1/2$, $p_2 = p_3 = 0$.

$\underline{D_3^7\ (R32),\ D_{3d}^5\ (R\bar{3}m),\ \text{and}\ D_{3d}^6\ (R\bar{3}6)}$

	X_0	Y_3
Δ_1	1	1
Δ_2	1	-1

Table 8

Matrix elements for propagation along a direction in the xz plane. Here $p_2 = p_3$. For Γ, $p_1 = p_2 = p_3 = 0$. For A, $p_1 = 1/2$, $p_2 = p_3 = 0$. For B, $p_1 = 0$, $p_2 = p_3 = -1/2$. For C_{3i}^2 ($R\bar{3}$) and D_3^7 (R32) the general propagation in the xz plane is not a symmetry direction.

$\underline{D_{3d}^5\ (R\bar{3}m)\ \text{and}\ D_{3d}^6\ (R\bar{3}c)}$

	X_0	Y_0
Even	1	1
Odd	1	-1

Table 9

Matrix elements and characters for the point A. Here $p_1 = 1/2$, $p_2 = p_3 = 0$.

C_{3i}^2 ($R\bar{3}$)

	X_0	X_3
A_1	1	1
A_2	1	-1

D_3^7 (R32)

	X_0	Y_3
A_1	1	1
A_2	1	-1

D_{3d}^5 ($R\bar{3}m$)

	X_0	X_3	Y_0	Y_3
A_1	1	1	1	1
A_2	1	1	-1	-1
A_3	1	-1	-1	1
A_4	1	-1	1	-1

D_{3d}^6 ($R\bar{3}c$)

	X_0	X_3	Y_0	Y_3
$(A_1)_{11}$	1	0	0	1
$(A_1)_{21}$	0	1	1	0
$(A_1)_{12}$	0	1	-1	0
$(A_1)_{22}$	1	0	0	-1
$\chi(A_1)$	2	0	0	0

Table 10

Matrix elements and characters for the point B. Here $p_1 = 0$, $p_2 = p_3 = -1/2$.

For C_{3i}^2 ($R\bar{3}$) and D_3^7 (R32) the symmetry situation is the same as at the point A. For D_{3d}^5 ($R\bar{3}m$) and D_{3d}^6 ($R\bar{3}c$), we have the same situation as for D_{3d}^5 ($R\bar{3}m$) at point A. The matrix elements are then as follows for these two cases:

	X_0	X_3	Y_0	Y_3
B_1	1	1	1	1
B_2	1	1	-1	-1
B_3	1	-1	-1	1
B_4	1	-1	1	-1

Table 11

Compatibility Relations

C_{3i}^2 ($R\bar{3}$)

Γ_1, Z_1	Γ_2, Z_2	Γ_3, Z_3	Γ_4, Z_4	Γ_5, Z_5	Γ_6, Z_6
Λ_1	Λ_3	Λ_2	Λ_2	Λ_3	Λ_1

D_3^7(R32)

Γ_1, Z_1	Γ_2, Z_2	Γ_3, Z_3	A_1	A_2
Λ_1	Λ_2	Λ_3	Δ_1'	Δ_2'

D_{3d}^5 ($R\bar{3}m$)

Γ_1, Z_1	Γ_2, Z_2	Γ_3, Z_3	Γ_4, Z_4	Γ_5, Z_5	Γ_6, Z_6
Λ_1	Λ_2	Λ_1	Λ_2	Λ_3	Λ_3
Δ_1	Δ_2	Δ_2	Δ_1	Δ_1, Δ_2	Δ_1, Δ_2

Table 11 (Continued)

$D_{3d}^5(R\bar{3}m)$ (continued)

A_1	A_2	A_3	A_4
Δ'_1	Δ'_2	Δ'_1	Δ'_2

D_{3d}^6 $(R\bar{3}c)$

Γ_1	Γ_2	Γ_3	Γ_4	Γ_5	Γ_6
Λ_1	Λ_2	Λ_1	Λ_2	Λ_3	Λ_3
Δ_1	Δ_2	Δ_2	Δ_1	Δ_1, Δ_2	Δ_1, Δ_2

Z_1	Z_2	Z_3
$\Lambda_1\Lambda_2$	Λ_3	Λ_3

A_1
Δ'_1, Δ'_2

Reference

1. G. F. Koster, Space Groups and their Representations, Solid State Physics, Vol. 1, p. 173, Academic Press Inc., New York, 1957.

BENZENE

Jules Moskowitz

The configuration interaction calculation based on the "core potential" approximation discussed in the past progress report has been slightly extended. The three center penetration integrals have been accurately computed rather than calculated by means of the Mulliken approximation. As anticipated, the basic results have not changed significantly. The more one improves the π electron wave function the worse the agreement with the experimental results. The $^3B_{1u}$ state, for example, is computed at 2.44 ev while the experimental value is 3.66 ev. The "core potential" approach thus seems to contain a fundamental defect.

A possible remedy would be the inclusion of the sigma electrons explicitly. This is fundamentally a data processing problem. A set of programs to perform the necessary calculations is in the process of being written. A self-consistent-field calculation on the benzene ground state would be the initial step in this approach.

AROMATIC AND RELATED MOLECULAR CALCULATIONS

B. T. Sutcliffe

As outlined in a previous QPR (No. 47, January 15, 1963, p. 116), calculations are being attempted on some molecular systems using the method of "Generalized Product" functions[1]. It is assumed that the "group" functions which go to make up a particular Generalized Product function are orthogonal in the "strong" sense of ref. [1] and are each composed of sets of one electron functions.

Programs have been written which, starting with integrals over an arbitrary basis of one electron functions, produce integrals over a suitably orthogonal basis. The minimum number of required integrals are produced and they are arranged in such a way that the elements of the effective Hamiltonian (see[1] eq. 25, p. 363) for each group in turn may be made up quickly and easily.

It is hoped shortly, to perform a pilot calculation on ethylene using Gaussian functions to obtain the basic integrals.

Reference

1. R. McWeeny, Rev. Mod. Phys. 32, 335, (1960).

THE POLYATOM SYSTEM

M. C. Harrison

The POLYATOM system of programs in its present preliminary form is capable of evaluating LCAO-SCF wavefunctions for a closed shell molecular system, expressed in terms of not more than 50 s and p-type Gaussian functions centered on not more than 20 nuclei. The various programs comprising the system communicate with each other via magnetic tape, on which data is stored in a specified format. It is convenient to crystalize this format at an early stage of development, so that programs using the same data may be written in parallel. Accordingly, the content and format of two of the magnetic tapes if given in detail below. It should be noted that the file-handling routines described briefly in CCL Technical Note 19 are used in referring to magnetic tape. This means essentially that each file of information is given a BCD name, and can be located on the tape when this name is known, whatever order the files may be in.

(1) Tape KMLIST

This tape is a logical unit 12, and contains 3 files, named K-LIST, V-LIST, and M-LIST. Given an ordered set of one-electron functions η_1, η_2, . . . η_n, with certain symmetry properties, these files contain labels of non-zero integrals of the types $(\eta_i|K|\eta_j)$, $(\eta_i|V|\eta_j)$, and $(\eta_i\eta_j|M|\eta_k\eta_\ell)$ where K is any totally summetric one-electron operator such as unity or $-1/2\,\nabla^2$, V is any operator having the symmetry of the nuclei such as $\Sigma_a \frac{1}{r_a}$, and M is any totally symmetric two-electron operator such as $\frac{1}{r_{12}}$. The indices in each label are given in standard order; that is, with $i \geq j$ in the one-electron cases and with $i \geq j$, $k \geq \ell$, and $(ij) \geq (k\ell)$ in the two-electron case, where $(ij) = i/2\,(i+1) + j$. The labels of integrals which are identically equal within a minus sign, because of the symmetry properties of the ηs, are given consecutively.

Each of the three files is divided into Fortran logical binary records, with the first word in each record being a Fortran integer not greater than 500 giving the number of labels in the record, the second a Fortran integer which is 1 if the record is the last in the file, and zero otherwise, and the remainder the labels, one in each word. Each word is divided into 6 fields, comprising bits s-5, 6-11, 12-17, 18-23, 24-29, 30-35. For the one electron integrals, fields 1, 2, and 6 are used to store i, j, and a tag respectively. For the two-electron integrals, fields 3 and 4 are used to store k and ℓ. The value of the tag is zero if the integral is not identically equal to any preceding integral, one if it is equal to the last integral with a zero tag, and two if it is equal to minus the last integral with a zero tag.

The ordering of the labels is such that the integrals which are equal within a minus sign are in standard order (that is, in increasing order of $((ij)\ (k\ell))$), and the integrals with zero tag are also in standard order.

(2) Tape KMINTS

This tape is a logical unit 11, and contains 4 files, named G-INTS, T-INTS, V-INTS, and M-INTS. These contain respectively the values of the overlap, kinetic energy, potential energy, and electronic repulsion integrals. Each file is divided into Fortran logical binary records, with the first two words in each file having the same meaning as in (1) above. The remainder of the record consists of the labels as before, but with each label followed by the value of the integral as a floating-point word. No assumptions should be made about field 6 of the label, however. It should not be assumed that there is only one integral for given values of the indices. Thus file V-INTS, for instance, may contain several entries for integral $(i|V|j)$, corresponding to different centres, which should be added together.

Note that the present format can only be used for up to 63 one-electron functions. Should this number be insufficient the tape format can easily be changed. However, preliminary tests on the 709 suggest that the computation time necessary for a larger basis set will be excessive.

MOLECULAR INTEGRALS OVER SLATER ORBITALS

D. E. Ellis

I. One and Two Center Integrals

A set of computer routines has been prepared by Mr. C. A. Christy and the author for the computation of all one and two center integrals arising in energy calculations using a basis of Slater orbitals. The one center integrals are computed from analytic formulae, and two center integrals are evaluated by the Barnett-Coulson method[2]. All angular integrations are carried out analytically. The radial integrations are performed by making use of the analytic series expansions for molecular zeta functions[3] $\zeta_{m,n}$, except for the exchange integrals, $<AB|AB>$. The $<AB|AB>$ integrals appear as an infinite series of radial integrals multiplied by angular coefficients, and these radial integrals are computed by means of Gauss-Legendre and Gauss-Laguerre quadratures[1].

Testing of the routines has been completed for combinations of 1s, 2s, 2p, and in some cases, 3d, orbitals. Results have been compared with the DIATOM program written by Switendick and Corbato[4], and with several other integrals programs. Further testing is planned.

Some comparison may be made with the DIATOM program, which has been in frequent use. The angular integrations proceed in much the same manner in both programs. DIATOM makes use of equal interval rule numerical integrations for all radial functions, including one center integrals. The analytic and Gauss integrations used in the routines being described permit higher accuracy and greater speed. The DIATOM program computes all non-zero integrals for a given basis set, and allows the basis set to be chosen as a linear combination of Slater orbitals. Sometimes only a few integrals, or integrals of a particular type are desired and it would be convenient to be

able to compute only those integrals. A very simple main program making use of the set of routines is being written for this purpose.

In the computation of a large number of integrals required, for example, in a self-consistent molecular calculation it becomes possible to decrease the computation time per integral very considerably by saving auxilliary functions from one integral to the next. As an example, exchange integrals requiring 1.5 minutes computation singly have been produced at an average rate of about 10 sec. apiece when a number are computed at once. Some function saving has been incorporated into the set of routines, and a main program is planned which will set up an efficient calculation of integrals over an entire basis.

II. Three Center Integrals

A computer routine has been written and partially tested for the evaluation of the three center nuclear repulsion integrals, $< AB \left| \frac{1}{rc} \right| >$. This routine, together with the routines described above, allow the computation of all integrals appearing in the one-electron Hamiltonian. Formulae have been derived for the two electron coulomb, $< AA \mid BC >$ and exchange $< AB \mid AC >$ integrals, and are being programmed. An integrals package is planned which will combine all routines under control of a main program for most efficient calculation.

III. Four Center Integrals

Elsewhere in this report Mr. J. P. Wright describes a program which he is writing to evaluate four center electron repulsion integrals between combinations of s, p, and d orbitals. We plan to co-ordinate the programs described above with this.

IV. Formulae

We want to sketch the derivation and give the formulae for a few of the integrals, but for the sake of brevity some steps and definitions will be omitted.

Define the normalized Slater orbital as

$$\phi = N\, r^{n-1}\, e^{-\kappa r} (-)^m P_\ell^m(\mu)\, S_m(\phi)$$

P_ℓ^m by Hobson's definition, $m \geq 0$

$$S_m^0(\phi) = \cos(m\phi) \qquad S_m^1(\phi) = \sin(m\phi)$$

and use the following expansions and definitions

$$r_b^{m-1} e^{-\kappa r_b} = \sum_{\lambda=0}^{\infty} (2\lambda+1)\zeta_{m,\lambda}(1,\kappa r_a, \kappa R)\, P_\lambda^0(\mu_a)$$

$$r_b^\ell P_\ell^m(\mu_b)\, S_m^\sigma(\phi_b) = \sum_{i=m}^{\ell} (-)^{i+m} \binom{\ell+m}{i+m} r_a^i R^{\ell-i} P_i^m(\mu_a) S_m^\sigma(\phi_a)$$

(z-axes antiparallel)

$$\frac{1}{r_{12}} = \sum_{j=0}^{\infty} \delta_j(r_{a_1}, r_{a_2})\, P_j^0(\mu_{12})$$

These relations prove sufficient for the derivation of all one and two center formulae, and the three center nuclear repulsion integral. It is assumed that the coordinate system on center A is right handed, and that system B is left handed, with z-axes antiparallel. To allow parallel co-ordinate axes in an absolute frame, and to compute the remaining three and four center integrals requires the introduction of the rotation matrices for solid harmonics. This we delay until a future report.

The method of derivation is to expand all functions onto center A, to couple the resulting Legendre functions, to expand products of trigonometric functions, and to perform the remaining angular integrals analytically. One important result is an expression for the potential integral

$$\langle AB \left| \frac{1}{r_{12}} \right| \rangle = \int \phi_1(A,1)\, \phi_2(B,1) \frac{1}{r_{12}}\, dv_1$$

$$= 2\pi N_1 N_2 \left(\frac{1}{\kappa_2}\right)^{n_1+n_2} \sum_{j=|m_1-m_2|}^{\infty} \frac{1}{2j+1} \sum_{i_2=m_2}^{\ell_2} (-)^{i_2+m_2} \binom{\ell_2+m_2}{i_2+m_2} (\kappa_2 R_b)^{\ell_2-i_2}$$

$$\sum_{\lambda_2} (2\lambda_2+1) \{\text{ang}\} \{\overline{zY}\}$$

where $$\left\{\text{ang}\right\} = \left\{(-)^{\sigma_1\sigma_2}\ {}^{\lambda_2,\ell_1,i_2}_{\ \ |m_1+m_2|}\ F_{j,m_1,-m_2}\ P_j^{|m_1+m_2|}(\mu_{a_2})\ S^{|\sigma_1-\sigma_2|}(\phi_{a_2})\right.$$

$$\left. + s^{m_1-m_2}\ (-)^{\sigma_1,\sigma_2}\ {}^{\lambda_2,\ell_1,i_2}_{\ \ |m_1-m_2|}\ F_{j,m_1,m_2}\ P_j^{|m_1-m_2|}(\mu a_2)\ S^{|\sigma_1-\sigma_2|}(\phi_{a_2})\right\}$$

(the F's are a sum of products of two D_ℓ's)

and $$\left\{\overline{zY}\right\} = \int_0^\infty e^{-\frac{\kappa_1}{\kappa_2}t}\ t^{n_1+i_2+1}\ \bar{\zeta}_{n_2-\ell_2,\lambda_2}(1, t, \kappa_2 R_b)\delta_j(t, \kappa_2\ r_{a_2})dt$$

To obtain the three center nuclear attraction integral, we merely set $r_{a_2} = R_c$, $\phi_{a_2} = \phi_c = 0$ $\mu_{a_2} = \mu_c$. The two center exchange integral is obtained as follows:

$$< AB\ \ AB > = \int < AB\ \frac{1}{r_{12}} > AB\ dv_2$$

and the result is

$$< AB\,|\,AB > = \delta_{|\sigma_1-\sigma_2|,\,|\sigma_3-\sigma_4|}\, E \sum_{j=|m_1-m_2|}^{\infty} \sum_{i_2=m_2}^{\ell_2} (-)^{i_2+m_2} \binom{\ell_2+m_2}{i_2+m_2} (\kappa_2 R_b)^{\ell_2-i_2}$$

$$\sum_{i_4=m_4}^{\ell_4} (-)^{i_4+m_4} \binom{\ell_4+m_4}{i_4+m_4} (\kappa_2 R_b)^{\ell_4-i_4} \sum_{\substack{\lambda_2,\lambda_4 \\ \text{finite}}} \frac{(2\lambda_2+1)(2\lambda_4+1)}{(2j+1)^2} \left\{\overline{zx}\right\}\left\{\text{ang}\right\}$$

where

$$\left\{\overline{zx}\right\} = \int_0 e^{-\frac{\kappa_3}{\kappa_2}s}\ s^{n_3+i_4+1}\ \bar{\zeta}_{n_4-\ell_4,\lambda_4}(1, \frac{\kappa_4}{\kappa_2}s,\ \kappa_4 R_b) \int_0 e^{-\frac{\kappa_1}{\kappa_2}t}\ t^{n_1+i_2+1}$$

$$\bar{\zeta}_{n_2-\ell_2,\lambda_2}(1, t, \kappa_2 R_b) * \delta_j(s, t)dtds$$

and $\left\{\text{ang}\right\}$ is a sum of four terms, each of which is a product of two F's and a factorial ratio.

References

1. M. P. Barnett, SSMTG Programming Notes No. 23, No. 38

2. M. P. Barnett and C. A. Coulson, Evaluation of Integrals Occurring in in the Theory of Molecular Structure, Phil. Trans. Roy. Soc., No. 864, Vol. 243, 1951

3. D. E. Ellis, SSMTG QPR No. 42, October 15, 1961

4. A. C. Switendick and F. J. Corbato, SSMTG QPR No. 34, October 15, 1959

FOUR-CENTER MOLECULAR INTEGRALS

J. P. Wright

Testing has begun of a program written to calculate four-center molecular integrals for any combination of s, p, and d functions with unrestricted principal quantum numbers. The zeta function method of Barnett and Coulson has been used. The formula for the general case has been derived using a notation similar to that given by D. E. Ellis in a report elsewhere in this QPR, where he discusses his work on three-center molecular integrals. The formula will be given in a future report, after testing has been completed.

EXPANSION THEOREMS FOR SOLID SPHERICAL HARMONICS

J. P. Dahl
M. P. Barnett

Some expansion theorems for solid spherical harmonics have been derived. It is hopeful that these theorems will prove to be useful in the calculation of three and four-center molecular integrals.

Consider the two coordinate systems a and b (Figure 1) with parallel axes. The location of b relative to a is specified by giving the vector $\vec{R} = (X, Y, Z) = (R, \Theta, \Phi)$, where the rectangular and spherical coordinates of $\vec{R}$ expressed in a have been denoted (X, Y, Z) and (R, Θ, Φ) respectively. With a similar notation a field point P may be specified by giving its coordinates in b, i.e. $\vec{r}_b = (x_b, y_b, z_b) = (r_b, \theta_b, \phi_b)$ or in a, $\vec{r}_a = (x_a, y_a, z_a) = (r_a, \theta_a, \phi_a)$. The relation

$$(x_b, y_b, z_b) = (x_a - X, y_a - Y, z_a - Z) \qquad (1)$$

obviously holds.

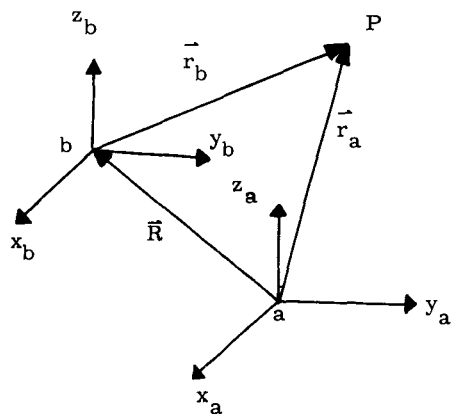

Figure 1

The following expansions are then valid:

$$r_b^N P_N^M(\cos\theta_b) \begin{cases} e^{iM\phi_b} \\ e^{-iM\phi_b} \\ \cos(M\phi_b) \\ \sin(M\phi_b) \end{cases} =$$

$$\sum_{n=0}^{N} \sum_{\substack{m= \\ n-N+M}}^{n} (-)^{N-n} \binom{N+M}{n+m} r_a^n R^{N-n} P_n^m(\cos\theta_a) P_{N-n}^{M-m}(\cos\Theta)$$

$$\begin{cases} e^{im\phi_a} e^{i(M-m)\Phi} & (2) \\ e^{-im\phi_a} e^{-i(M-m)\Phi} & (3) \\ \cos[m\phi_a + (M-m)\Phi] & (4) \\ \sin[m\phi_a + (M-m)\Phi] & (5) \end{cases}$$

The associated Legendre functions are those defined by Hobson[1]

$$P_n^m(\cos\theta) = (-)^m \sin^m\theta \frac{d^m}{d(\cos\theta)^m} P_n(\cos\theta), \quad m \geq 0 \qquad (6)$$

$$P_n^{-m}(\cos\theta) = (-)^m \frac{(n-m)!}{(n+m)!} P_n^m(\cos\theta) \qquad (7)$$

The relation (7) holds for all m values. Further it follows from (6) that $P_n^m(\cos\theta) = 0$ for $|m| > n$.

The coefficients $\binom{N+M}{n+m}$ occurring in (2) - (5) are the binomial coefficients, i.e.:

$$\binom{p}{g} = \frac{p!}{g!(p-g)!}$$

It suffices to demonstrate the validity of (2), since (3) is merely the complex conjugate of (2). Further (4) and (5) are obtained from equations (2) and (3) simply by adding and subtracting these two equations.

From the defining equation (6) it follows that

$$P_n^n(\cos\theta) = (1)^n \frac{(2n)!}{2^n n!} \sin^n\theta$$

or:

$$r^n P_n^n(\cos\theta)\, e^{in\phi} = (-)^n \frac{(2n)!}{2^n n!} (x+iy)^n \qquad (8)$$

Considering Eq. (1) we then obtain

$$r_b^N P_N^N(\cos\theta_b)\, e^{iN\phi_b} = (-)^N \frac{(2N)!}{2^N N!} [(x_a+iy_a) - (X+iY)]^N$$

$$= (-)^N \frac{(2N)!}{2^N N!} \sum_{n=0}^{N} (-)^{N-n} \binom{N}{n} (x_a+iy_a)^n (X+iY)^{N-n}$$

or:

$$r_b^N P_N^N(\cos\theta_b)\, e^{iN\phi_b} = \sum_{n=0}^{N} (-)^{N-n} \binom{2N}{2n} r_a^n R^{N-n} P_n^n(\cos\theta_a)\, P_{N-n}^{N-n}(\cos\Theta)$$

$$e^{in\phi_a}\, e^{i(N-n)\Phi} \qquad (9)$$

Equation (9) is obviously identical with equation (2) in the case M=N. Equation (2) has thus been shown to hold for the maximum value which M can take. From the process of induction it follows that the equation is valid in general, if validity for M implies validity for the value M-1.

Suppose therefore that (2) holds for the value M. We then consider simultaneous, infinitesimal rotations of the coordinate systems a and b through the same angle about parallel axes. The changes in the functions involved are then found by applying the operators of angular momentum, since these operators are proportional to the operators for small rotations. The fact that r_a, r_b and R are all rotated through the same angle then implies that operating with an angular momentum operator $\hat{\ell}_b$ on the left hand side of Eq. (2) is equivalent to operating with the operator $\hat{\ell} + \hat{\ell}_a$ on the right hand side. Here ℓ and ℓ_a are the same functions of (Θ, Φ) and (θ_a, ϕ_a) as $\hat{\ell}_b$ is of (θ_b, ϕ_b).

From the well known properties of the operator $\hat{\ell}_x - i\hat{\ell}_y$ it follows that

$$(\hat{\ell}_x - i\hat{\ell}_y)\, P_n^m(\cos\theta)\, e^{im\phi} = (n+m)(n-m+1) P_n^{m-1}(\cos\theta)\, e^{i(m-1)\phi} \qquad (10)$$

Operating on the left hand side of Eq. (2) with the operator $\hat{\ell}_{x_b} - i\hat{\ell}_{y_b}$ and on the right hand side with the operator $(\hat{\ell}_X - i\hat{\ell}_Y) + (\hat{\ell}_{x_a} - i\hat{\ell}_{y_a})$ we obtain:

$$(N+M)(N-M+1) r_b^N P_N^{M-1}(\cos\theta_b)\, e^{i(M-1)\phi_b} =$$

$$\sum_{n=0}^{N} \sum_{\substack{m= \\ n-N+M}}^{n} (-)^{N-n} \binom{N+M}{n+m} (n+m)(n-m+1)\, r_a^n R^{N-n}$$

$$P_n^{m-1}(\cos\theta_a) P_{N-n}^{M-m}(\cos\Theta) e^{i(m-1)\phi_a} e^{i(M-m)\Phi}$$

$$+ \sum_{n=0}^{N} \sum_{\substack{m= \\ n-N+M}}^{n} (-)^{N-n} \binom{N+M}{n+m} (N+M-m-n)(N-M-n+m+1)\, r_a^n R^{N-n}$$

$$P_n^m(\cos\theta_a)\, P_{N-n}^{M-m-1}(\cos\Theta)\, e^{im\phi_a} e^{i(M-m-1)\Phi}$$

Writing m for m-1 in the first summation on the right hand side it is readily shown that this equation may be rewritten as

$$r_b^N P_N^{M-1}(\cos\theta_b)\, e^{i(M-1)\phi_b} =$$

$$\sum_{n=0} \sum_{\substack{m= \\ n-N+M-1}} (-)^{N-n} \binom{N+M-1}{n+m} r_a^n R^{N-n}$$

$$P_n^m(\cos\theta_a)\, P_{N-n}^{M-m-1}(\cos\Theta)\, e^{im\phi_a} e^{i(M-m-1)\Phi}$$

which is just Eq. (2) for the value M-1.

The general validity of the equations (2) - (5) has thus been demonstrated.

After completion of the present work it has come to our attention that an equation similar to Eq. (2) has been derived by M. E. Rose (J. Math. and Phys. 37, 215 (1958)), who applied the algebra of irreducible tensors. The equation appeared as a subordinate result in a study of the electrostatic interaction of two charge distributions. Rose presented his equation in the form:

$$\mathcal{Y}_N^M(\vec{r}_b) = (4\pi)^{1/2} [(2N+1)!]^{1/2}$$

$$\sum_{n=0}^{N} \sum_{m=-n}^{n} \frac{(-)^n \mathcal{C}(n, N-n, N; m, M-m)}{[(2n+1)!(2N-2n+1)!]^{1/2}} \mathcal{Y}_n^m(\vec{R})\, \mathcal{Y}_{N-n}^{M-m}(\vec{r}_a)$$

where $\mathcal{Y}_n^m(\vec{r})$ is a normalized solid spherical harmonic:

$$\mathcal{Y}_n^m(\vec{r}) = (2\pi)^{-1/2}\left[\frac{2n+1}{2}\,\frac{(n-m)!}{(n+m)!}\right]^{1/2} r^n P_n^m(\cos\theta)\, e^{im\phi}$$

and the C-coefficients are vector addition coefficients. By substituting the actual form of these coefficients into Rose's equation the equivalence with equation (2) could be demonstrated.

References

1. E. W. Hobson, Theory of Spherical and Ellipsoidal Harmonics, Cambridge University Press, 1931.

MONTE CARLO METHOD FOR MOLECULAR INTEGRALS

C. W. Nielson
B. J. Woznick

The Monte Carlo method has been widely used for solving problems in neutron kinetics and has sporadically been used for the evaluation of multi-dimensional integrals for other purposes[1, 2, 3, 4]. We are investigating the possible usefulness of this method for the evaluation of multicenter molecular integrals.

The advantages of this method are its extreme simplicity, the fact that it is not limited to any special type of orbital functions, and the fact that it provides automatically an estimate of the error. However, Monte Carlo calculations are almost certain to take much longer for comparable accuracy than methods which make special use of the analytic properties of the functions involved, such as the zeta-function expansion method or the Gaussian transform method. Nevertheless, it seems that the Monte Carlo approach has real value for the evaluation of integrals involving unusual functions, perhaps numerical, and also for the checking of other methods as they are extended into new domains. In addition, the simplicity of the method makes it feasible to implement it on very small computers.

The basis of the method may be seen by considering the definition of an integral as

$$\int_a^b f(x)dx = \lim_{\substack{n\to\infty \\ \Delta xk\to 0}} \sum_{k=1}^{n} f(x_k^*)\,\Delta xk \qquad (1)$$

where $\Delta x_k = x_{k+1} - x_k$ and x_k^* is some point in this interval. Then, if the intevals are chosen to be equal and the limits taken as 0 and 1,

$$\int_0^1 f(x)dx = \lim_{n\to\infty} \frac{1}{n} \sum_{k=1}^{n} f(x_k^*) \qquad (2)$$

where the x_k^* are distributed uniformly in the interval 0-1. Ordinary techniques of integration achieve this uniform distribution by chopping the interval into n equal subintervals. The essence of the Monte Carlo method is to choose these points at random; in this context, "at ramdom" simply means that we have a set of points which are uniformly distributed and statistically independent.

There is, of course, no value in doing this for one-dimensional integrals. However, theorems of probability theory have been proven which show that the probable error in the integral goes down as $1/\sqrt{N}$ regardless of the dimensionality. In contrast, straightforward numerical integration requires the number of points to increase geometrically with the dimension. For a sixfold integration such as occurs in molecular integrals, straightforward numerical integration seems out of the question, whereas Monte Carlo integration does not.

Another important tool in making the technique practicable is the use of a distribution function, or weighting factor. Assume that the integrand can be written as the product of two factors

$$I = \int_a^b f(x)\, g(x)\, dx \tag{3}$$

where

$$\int g(x)\, dx = 1 \tag{4}$$

and g(x) is everywhere non-negative. Then we can take this function to be a probability density and select the points x_i^* according to this distribution. This having been done,

$$\int f(x)\, g(x)\, dx = \lim_{N\to\infty} \frac{1}{N} \sum_1^n f(x_k^*) \tag{5}$$

Qualitatively, this procedure can be looked upon as dividing out an exactly integrable part of the integrand leaving a more smoothly varying function to integrate numerically. If the distribution function is chosen appropriately, the numerical integration points are taken only where the integrand is significant, hence the technique is sometimes called importance sampling.

We have used these methods to calculate four-center molecular integrals using 1S orbitals on all centers. The distribution function used was a product of two three-dimensional factors, one for each of the two electronic coordinates systems of the molecular integral. Each factor was a spherically symmetric function centered somewhere in the molecule. The radial part of the function was a constant inside a radius characteristic of the molecule and of the form $\frac{e^{-\tau r}}{r^2}$ outside this radius where τ was chosen to match the

assymptotic form of the orbitals. This function is suitable for a distribution function because it can be integrated exactly and thus normalized. Random numbers uniform in the unit hypercube are generated on the computer by standard algorithms; these are more properly called pseudo-ramdom numbers, since they are in fact generated by an exact algorithm. They do, however, share most of the mathematical properties of random numbers. The uniform distribution was transformed by a "stretching" process subject to the requirement

$$\int_0^{\rho} d\tau = \int_0^{r} f(r')\, d\tau \qquad (6)$$

where ρ is the radius in the unit sphere and r is the radius in the final distribution. (Points falling outside the unit spheres are discarded.)

As an example of the results, a typical integral was obtained using 5000 random points as $.35 \pm .01$ whereas the zeta-function programs available give in a comparable time 0.36735, a value believed to be correct to all of the figures given. The Monte-Carlo computer program required for this calculation is extraordinarily short compared to the zeta-function program system. Also, negligible amounts of temporary storage are needed. Thus it is demonstrated that integrals of limited accuracy can be obtained very simply by this method. However, in view of the fact that the Monte-Carlo error would decline only as $1/\sqrt{N}$, accuracy comparable to the zeta-function method is practically impossible.

Recently Haselgrove[5] has suggested using so called diophantine numbers in a fashion similar to the random numbers in the Monte-Carlo method. These numbers also tend towards filling space uniformly, but with less fluctuation from uniformity than random numbers. His claim is that the error in an integral in this case goes down as $1/N$ rather than $1/\sqrt{N}$ as in the Monte Carlo case. We are now investigating the application of these diophantine numbers to the evaluation of molecular integrals.

References

1. H. Kahn, Multiple Quadrature by Monte Carlo methods in Mathematical Methods for Digital Computers, A. Ralston (ed.), John Wiley and Sons, New York, 1960.

2. H. A. Mayer, (ed.), Symposium on Monte Carlo Methods, John Wiley and Sons, New York, 1956.

3. H. Kahn, Applications of Monte Carlo, Research Memorandum RM-1237-AEC, The RAND Corporation, Apr. 19, 1954.

4. M. Gell-Mann and K. A. Brueckner, Correlation Energy of an Electron Gas at High Density, Phys. Rev., 106, Apr 15, 1957, eq. 9.

5. C. B. Haselgrove, A Method for Numerical Integration, Mathematics of Computation, October 1961, p. 323.

THE QUADRATIC JAHN-TELLER EFFECT

Don E. Ellis
Robert Englman

The ground-state energy expectation values have been computed, as functions of the strength of the linear interaction (k) and the quadratic coupling (ℓ), from the Hamiltonian and the approximate solution given in an earlier report[1]. The questions that the computation was designed to answer were:

(1) What is the effect of the quadratic coupling on the stabilization of the system (i.e., on the lowering of the ground state energy compared to the energy of an uncoupled system)?

(2) Is any analytic expression suggested by the results?

(3) What is the nature of the splitting of the lowest pair, which is degenerate in the linear effect (ℓ=0)? In particular,

(4) What is the balance of the effects on the upper of the pair of the upward tendency of the splitting and of the downward tendency of stabilization, and

(5) Where does this level meet the second harmonic?

Figures 1-4 provide the answer. It is important to note that the figures are plotted as though curves with different ℓ's coincided in k=0. This is not the case, since the zero-point motion energies are $\frac{1}{2}(\sqrt{1+\ell}+\sqrt{1-\ell})$ for k=0. This slowly varying quantity should then be added to the value of the curve to obtain the energy.

Regarding question (2), the plotted stabilized energy can be represented by $-\frac{1}{2}k^2/(1-\ell)+0(1)$ for large k and any ℓ. No simple expression

was found for the upper of the pair in this limit. However, an analytic, exact expression was derived by second-order perturbation theory and valid up to the order of k^2 (for small k) and any ℓ for both of the pair. The expression is involved. For ℓ small it reduces to $-k^2/(1-\ell)$ for the lower of the pair and $-k^2/(1+\ell)$ for the upper ($\ell>0$).

Figure 4 is purported to answer (5). Our method applies only to the ground-state pair and cannot give the level of the second harmonic. However, we have reason to expect that the separation of this level from the lowest one varies only weakly with k, ℓ and can be taken as 1.

The table gives numerical results for comparison with future computations. Our computations were carried out on the IBM 709 by means of numerical quadrature of complicated formulae. Characteristically, a thousand values were computed on a rectangular mesh, a pair of energies was obtained in 2 minutes.

The importance of this work may be seen by the light of the fact that after the initial impetus of the Jahn-Teller effect in 1957-8, progress has slowed down and, in terms of exact results, virtually halted, ostensibly because of the difficulties in obtaining exact solution. Regarding the reliability of our results, based as they are on approximate formulae, we are confident that they reproduce faithfully any qualitative aspect and suffice, at this stage, for comparison with the experiments that one would think of.

We are thankful to Professor W. Thorson for directing our attention to this work.

Table 1

Numerical Level Heights for $\ell = 0.5$

k =	0.3	0.5	1.0	2.0
Upper	-0.009714	-0.227310	+0.71908	+16.4301
Lower	-0.108763	-0.301881	-1.12986	-4.1443

References

Robert Englman, Quarterly Progress Report No. 46 of Solid-State and Molecular Theory Group, M.I.T., p. 158 (1962)

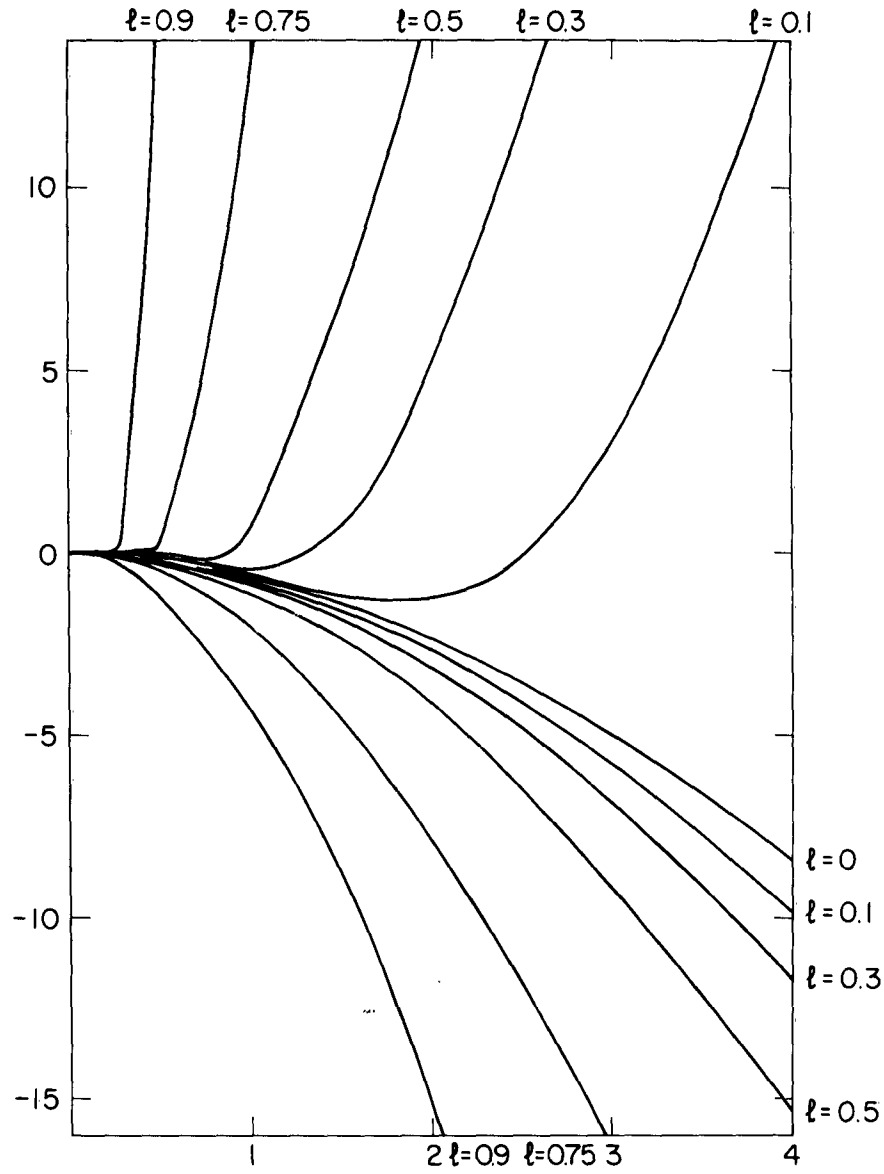

Figure 1

Energy vs. k (the linear coupling strength) with ℓ (the quadratic coupling strength) as parameters. The drooping curves are the ground-state energies; the rising ones belong to the upper of the ground-state pair.

(Note the sliding zero of the ordinate. Add $\frac{1}{2}(\sqrt{1+\ell} + \sqrt{1-\ell})$ to obtain energy.)

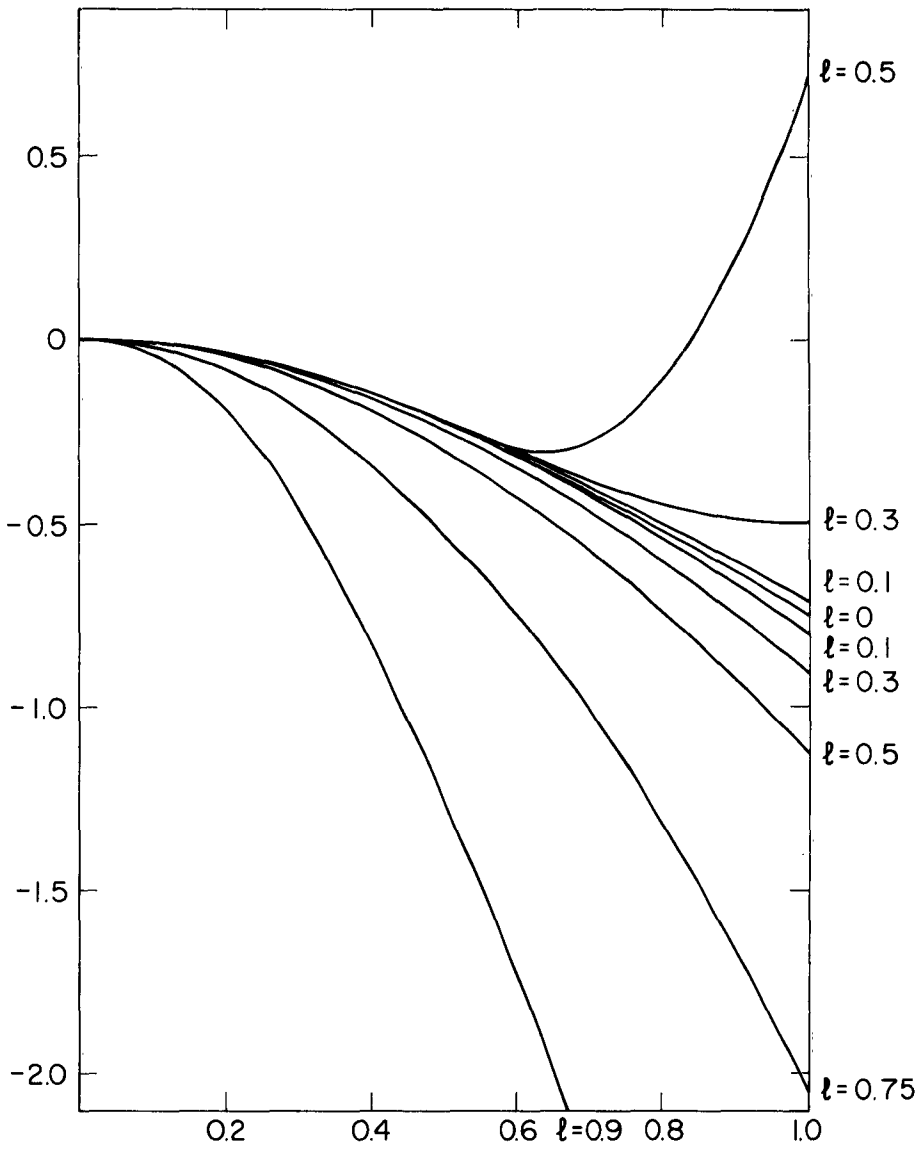

Figure 2

Enlargement of Figure 1 for small k

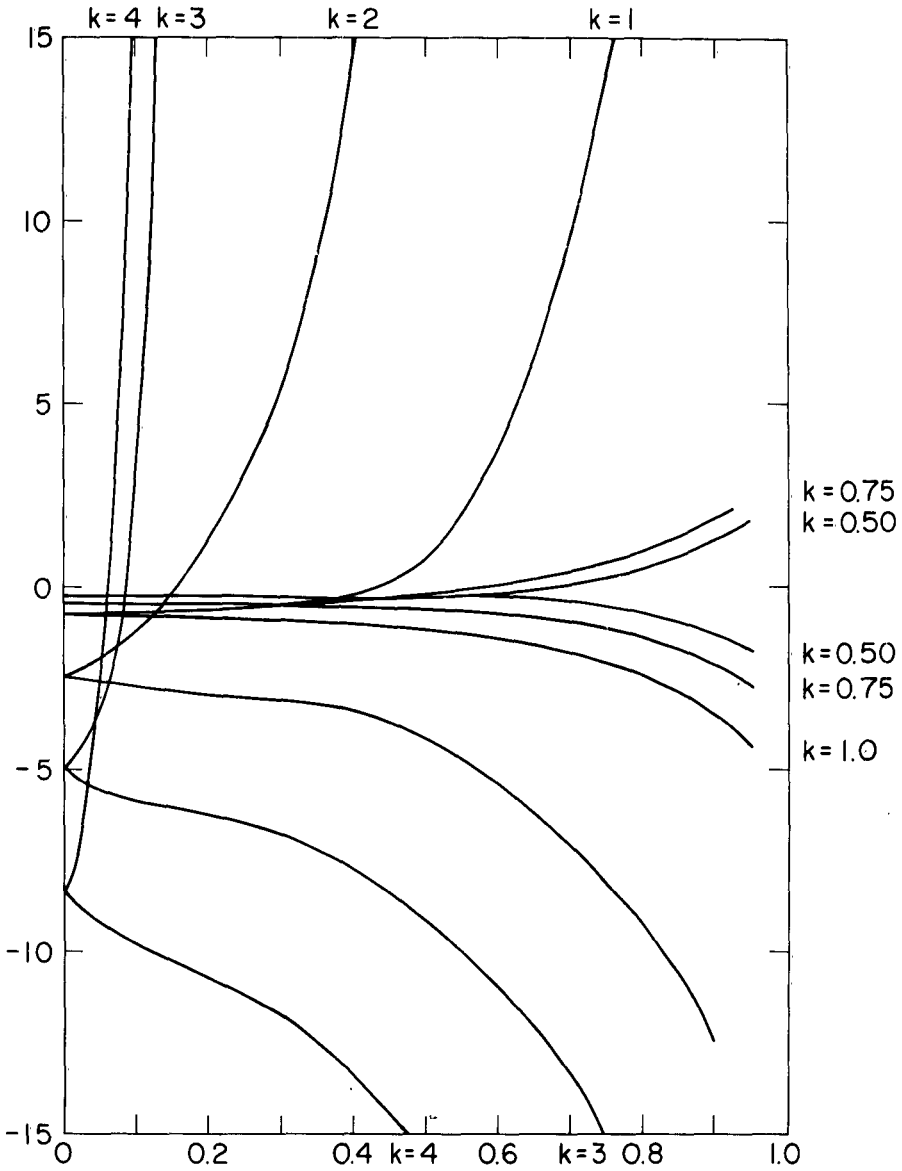

Figure 3

Energy vs. ℓ with k as parameters

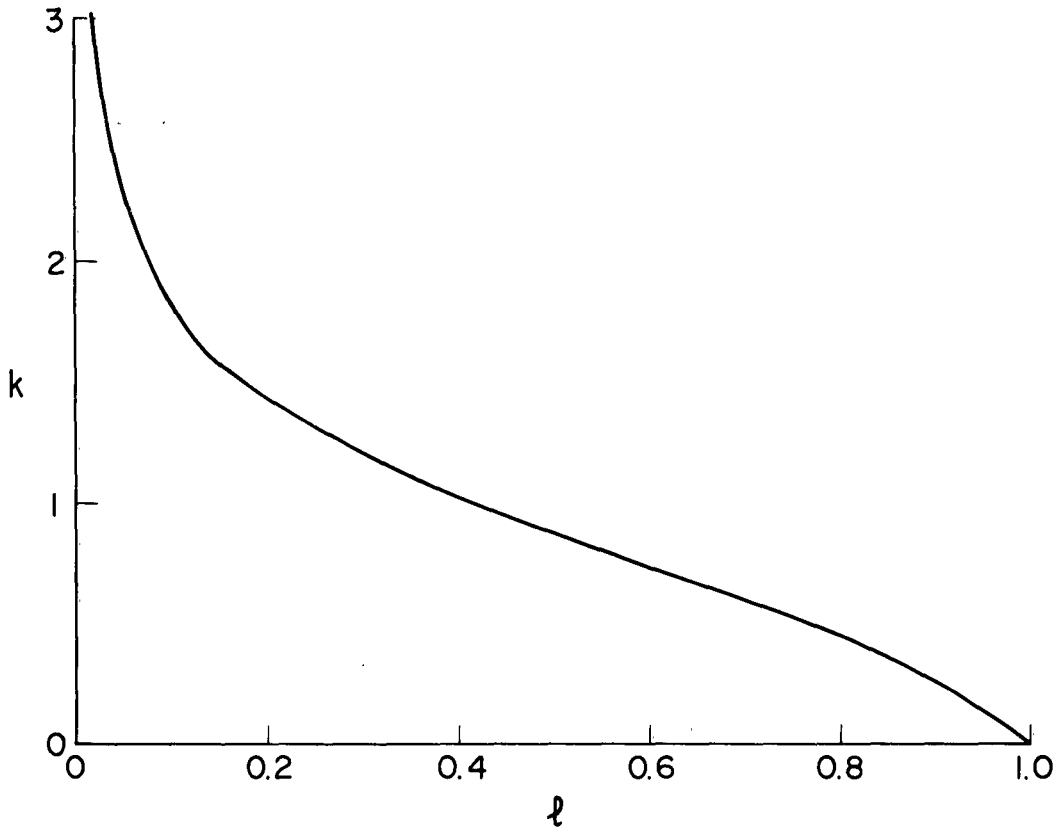

Figure 4

The value of k such that the splitting of the ground-state pair levels is 1, plotted vs. ℓ. At the plotted points (ℓ, k) the upper level coincides approximately with the second harmonic of the ground state.